Available online at www.sciencedirect.com
ScienceDirect
Advanced Drug Delivery Reviews 59 (2007) 1413–1433
Advanced DRUG DELIVERY Reviews
www.elsevier.com/locate/addr

Nanofiber technology: Designing the next generation of tissue engineering scaffolds ☆

Catherine P. Barnes [a], Scott A. Sell [a], Eugene D. Boland [a], David G. Simpson [b], Gary L. Bowlin [a,*]

[a] *Department of Biomedical Engineering, Virginia Commonwealth University, Richmond, VA 23284-3067, USA*
[b] *Department of Anatomy & Neurobiology, Virginia Commonwealth University, Richmond, VA 23298-0709, USA*

Received 14 December 2006; accepted 16 April 2007
Available online 25 August 2007

Abstract

Tissue engineering is an interdisciplinary field that has attempted to utilize a variety of processing methods with synthetic and natural polymers to fabricate scaffolds for the regeneration of tissues and organs. The study of structure–function relationships in both normal and pathological tissues has been coupled with the development of biologically active substitutes or engineered materials. The fibrillar collagens, types I, II, and III, are the most abundant natural polymers in the body and are found throughout the interstitial spaces where they function to impart overall structural integrity and strength to tissues. The collagen structures, referred to as extracellular matrix (ECM), provide the cells with the appropriate biological environment for embryologic development, organogenesis, cell growth, and wound repair. In the native tissues, the structural ECM proteins range in diameter from 50 to 500 nm. In order to create scaffolds or ECM analogues, which are truly biomimicking at this scale, one must employ nanotechnology. Recent advances in nanotechnology have led to a variety of approaches for the development of engineered ECM analogues. To date, three processing techniques (self-assembly, phase separation, and electrospinning) have evolved to allow the fabrication of nanofibrous scaffolds. With these advances, the long-awaited and much anticipated construction of a truly "biomimicking" or "ideal" tissue engineered environment, or scaffold, for a variety of tissues is now highly feasible. This review will discuss the three primary technologies (with a focus on electrospinning) available to create tissue engineering scaffolds that are capable of mimicking native tissue, as well as explore the wide array of materials investigated for use in scaffolds.

Keywords: Nanofibers; Electrospinning; Tissue engineering; Scaffold

Contents

☆ Disclosure: Several authors have patents pending concerning technology presented in this manuscript and this technology has been licensed to NanoMatrix, Inc. of which several authors have a financial interest. The early work in developing electrospinning tissue engineering scaffolds has been funded by The Whitaker Foundation (RG-98-0465 and TF-02-0013).

* Corresponding author. Department of Biomedical Engineering, Virginia Commonwealth University, P.O. Box 843067, Richmond, VA 23284-3067, USA. Tel.: +1 804 828 2592; fax: +1 804 828 4454.
E-mail address: glbowlin@vcu.edu (G.L. Bowlin).

0169-409X/$ - see front matter © 2007 Elsevier B.V. All rights reserved.
doi:10.1016/j.addr.2007.04.022

1. Introduction

Tissue engineering, or regenerative medicine, is an interdisciplinary field that merges principles and innovations from engineering and life sciences for the purpose of addressing the improvement, repair, or replacement of tissue/organ function [1,2]. Since its inception, the field has been governed by the generic concept of combining cell, scaffold (artificial extracellular matrix), and bioreactor technologies in the design and fabrication of neo-tissues/organs. This is logical since every tissue or organ in our body is composed of parenchymal cells (functional cells) and mesenchymal cells (support cells) contained within an extracellular matrix (ECM) to form a microenvironment. These microenvironments collectively form our tissues and organs. In terms of development and maintenance of the tissues and organs, our body is the "bioreactor", exposing the cell and ECM microenvironments to biomechanical forces and biochemical signals.

Composition (*i.e.*, biomaterials of synthetic or natural origin) and architecture of a tissue engineered scaffold result in cell–environment interactions that determine the structure's fate. The ultimate goal is to enable the body (cellular components) to heal itself by introducing a tissue engineered scaffold that the body recognizes as "self", and in turn, uses to regenerate "neo-native" functional tissues. It has long been hypothesized that in order to duplicate all of the essential intercellular reactions and promote native intracellular responses, the ECM must be mimicked. These synthetic ECMs or scaffolds must be designed to conform to a specific set of requirements. The first requirement is that the material be biocompatible and function without interrupting other physiological processes. This functionality includes an ability to promote normal cell growth and differentiation while maintaining a three-dimensional orientation/space for the cells. Secondly, the scaffold must not promote or initiate any adverse tissue reaction [3]. In addition, for clinical and commercial success, scaffold production must be simple yet versatile enough to produce a wide array of configurations to accommodate the size, shape, strength, and other intricacies of the target tissue/organ [3–7]. Once implemented *in vitro* or *in vivo*, the material must either be removed via degradation and absorption or incorporated via innate remodeling mechanisms, leaving only native tissue. Beyond these generalized requirements, we must look at the way a single native cell interacts with its immediate surroundings. It is no longer acceptable to view a cell as a self-contained unit residing in a passive structural network. Rather, a dynamic three-dimensional inter-relation is constantly kept in balance and influenced by both internal and external stimuli. Thus, any scaffold material must be able to interact with cells in three dimensions and facilitate this communication. In the native tissues, the structural ECM proteins (50–500 nm diameter fibers) are 1 to 2 orders of magnitude smaller than the cell itself; this allows the cell to be in direct contact with many ECM fibers, thereby defining its three-dimensional orientation. This property may be a crucial factor in determining the success or failure of a tissue engineering scaffold. In summary, the environmental conditions of a successful tissue engineered scaffold must be appropriate such that signals can be exchanged between cells and between cells and the environment with the goal of restoring tissue function.

Scientists in tissue engineering have turned to nanotechnology, specifically nanofibers, as the solution to the development of tissue engineering scaffolds and wound repair/care products. At present, only a few processing techniques can successfully produce fibers, and subsequent scaffolds, on the nanoscale [8,9]. Characterization of these nanofibrous structures for tissue engineering applications is crucial in understanding the cell–ECM interactions. This paper provides a review of the processing techniques, characteristics, and advantages of nanofibers in tissue engineering and the synthetic and natural polymers electrospun for tissue engineering applications.

2. Processing of nanofibers for tissue engineering

Conventional polymer processing techniques have difficulty in producing fibers smaller than 10 μm in diameter, which are several orders of magnitude larger than the native ECM (50–500 nm). For this reason, there has been a concerted effort to develop methods of producing nanofibers to more adequately simulate the ECM geometry. Three distinct techniques have proven successful in routinely creating nanofibrous tissue engineering structures: self-assembly, phase separation, and electrospinning [8–11].

Self-assembly involves the spontaneous organization of individual components into an ordered and stable structure with preprogrammed non-covalent bonds [8–14]. While a common natural process responsible for several essential biological components (nucleic acid synthesis, protein synthesis, and energy transduction), self-assembly is a rather complex laboratory procedure that is limited to only a select few polymer

configurations (diblock copolymers, triblock copolymers, triblocks from peptide-amphiphile, and dendrimers) [8]. The most common of these for the production of nanoscale fibers are the peptide-amphiphiles (PA). The work by Hartgerink et al. on bone tissue engineering has shown that these PAs perform best when they are specifically tailored to include several critical structural features, namely a long alkyl tail for hydrophobicity, four consecutive cysteine residues to create disulfide bonds for polymerization, and a linker region of three glycine residues to provide flexibility to the hydrophilic head group [9,12,14]. When placed in water, the hydrophobic alkyl tail groups will cluster together to form a cylindrical micelle with the hydrophilic head group exposed. These PAs will then be subjected to acid induced self-assembly (Fig. 1). This involves treating the PA solution with a dithiothreitol solution at a pH of 8, where the PA remains water soluble, and then reducing the pH to 4 and rapidly making the fibers insoluble. This technique generally creates nanofibers 5–8 nm in diameter and 1 μm in length. Other self-assembly methods include divalent ion induced self-assembly (addition of Ca^{2+} ions to cause gelation of the solution) and drying on surfaces (simply allowing the pH 8 water solution to dry on a surface) [9,11,12,14]. While each of the self-assembly techniques successfully yields nanofibers that are consistently on the small end of the natural ECM scale, the complexity of the procedure and the low productivity of the method limit it as a large-scale tissue engineering option [11].

Phase separation has been used for several years as a technique to create porous polymer membranes. However, Ma and Zhang pioneered the use of this technique as a means to produce nanofibrous, three-dimensional scaffolds whose macroporous architecture can be tailored to suit individual needs (reported porosities as high as 98.5%). These scaffolds can be created from a variety of biodegradable aliphatic polyesters, and are composed of fibers with diameters that range from 50 to 500 nm (nearly identical to that of natural collagen in the ECM) [8,9,11,15–17]. Phase separation is a thermodynamic separation of a polymer solution into a polymer-rich component and a polymer-poor/solvent-rich component. Essentially, a polymer is dissolved in solution and the phase separation is induced, either thermally (most common method) or through the addition of a nonsolvent to the polymer solution to create a gel. Water is then used to extract the solvent from the gel; the gel is cooled to a temperature below the glass transition temperature of the polymer and freeze dried under vacuum to produce a nanofibrous scaffold [8,9,11]. The macroporous architecture can be controlled through the addition of various porogens (*i.e.*, sugar, inorganic salt, paraffin spheres) to the polymer solution during the phase separation process (Fig. 2). This provides scaffold engineers with a significant amount of control in tailoring both the pore sizes and interconnectivity by altering the concentration, size, and geometry of the porogens used [9]. Unlike self-assembly, phase separation is a simple technique that does not require much specialized equipment. It is also easy to achieve batch-to-batch consistency, and tailoring of scaffold mechanical properties and architecture is easily achieved by varying polymer/porogen concentrations. However, this method is limited to being effective with only a select number of polymers and is strictly a laboratory scale technique [8].

Electrospinning is a process that was first conceived in the late 19th century by Lord Rayleigh, with the first US patent being issued in 1934 to Formhals [18,19]. Since that time little about the process has changed. In its simplest form, electrospinning essentially consists of the creation of an electric field between a grounded target and a positively charged capillary filled with a polymer solution (Fig. 3). When the electrostatic charge becomes larger than the surface tension of the polymer solution at the capillary tip, a polymer jet is created. This fine polymer jet travels from the charged capillary to the grounded mandrel and allows for the production of continuous micro- to nanoscale polymer fibers, which can be collected in various orientations to create unique structures in terms of composition and mechanical properties [8–11,18,20–24].

Having been utilized sporadically since its conception as a method for manufacturing textiles, this simple technique has, in the past decade or so, piqued the interests of many tissue engineers. This is due in part to the simplicity of the process and also to the diversity and control over scaffold geometries and mechanical characteristics that it affords the user. The entire technique can be performed with a minimal amount of specialized laboratory equipment; yet it can be modified to successfully create three-dimensional scaffolds of a variety of polymers [8,24]. Our lab has effectively electrospun the biodegradable polymers poly (glycolic acid) (PGA), poly(lactic acid) (PLA), copolymers and blends of PGA and PLA, poly(ε-caprolactone) (PCL), and polydioxanone (PDO), as well as the natural polymers collagen (types I, II, III, and IV), gelatin, elastin, fibrinogen, hemoglobin, and myoglobin. In addition, mixing solutions of these synthetic and natural polymers is possible, and has been performed in our lab to develop novel biomedical textiles, including tissue engineering scaffolds, vascular grafts, wound dressings, and hemostatic bandages. It is also possible to electrospin the components simultaneously from separate solutions (resulting in one layer), or to create a layered scaffold by sequentially electrospinning any number of polymer solutions [3].

The adjustment of several electrospinning parameters allows for further control and refinement of scaffold characteristics [21,23,25]. Altering the concentration/viscosity of the polymer solution affects fiber diameter: the higher the concentration, the larger the diameter of the fibers. Varying the geometry of the grounded target will change the size and shape of the electrospun scaffold. Scaffold thickness is dependent on the volume of polymer solution to be electrospun; greater volumes equate to thicker specimens. Fiber alignment is controlled by rotation of the grounded target. A high rotational speed will draw the fibers into a highly aligned formation parallel to the direction of rotation, while low rotational speeds allow the fibers to collect randomly on the grounded target.

As mentioned previously, a major attraction of electrospinning is its simplicity. This simplicity allows for electrospinning to be the only nanofibrous processing technique that can be taken out of a laboratory setting and be utilized successfully in scale-up and mass production [8]. Yet opponents of the process point out that despite the simplicity, diversity, and control offered by electrospinning, it is not a perfect solution to the creation of nanofibrous ECM analogues. For example, the diameters of electrospun fibers

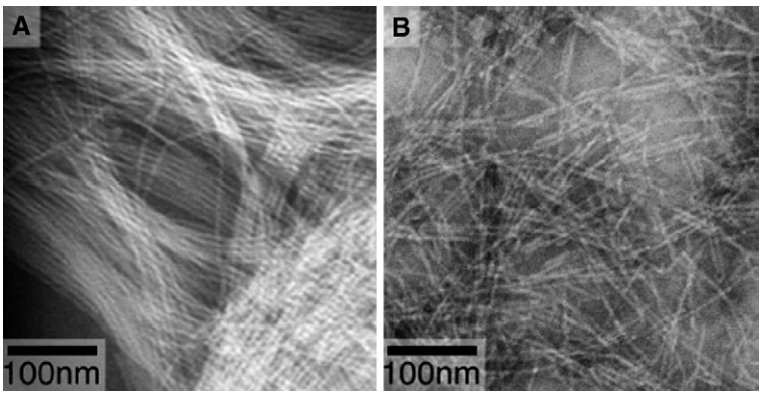

Fig. 1. Transmission electron microscopy images of nanofibers created through acid induced self-assembly of two different molecules with the same peptide sequence. The fibers are 1 μm long and 5–8 nm in diameter. Reprinted from [14], copyright 1993–2005 by The National Academy of Science of the United States of America, all rights reserved.

generally reside on the upper limits of the natural ECM's 50–500 nm range. Depending on the polymer to be electrospun, and its concentration, these fibers may even end up as micron scale in diameter. Also, electrospinning creates randomly interconnected void spaces throughout a scaffold. There is currently little to no way of creating a uniform, controlled, three-dimensional pore structure that can be incorporated into an electrospun scaffold [9].

Since there is no consensus on the gold standard for creating analogues to the native ECM, all three and even combinations of these processing techniques have been utilized to produce nanofibrous structures. For example, Bognitzki et al. used both electrospinning and phase separation to create sub-micron diameter fibers with pores or pits on the order of 100 nm [26]. Table 1 gives a summary of the advantages and limitations of each processing technique previously described. The authors of this review utilize electrospinning to produce tissue engineering scaffolds in the laboratory, and believe that the cost effectiveness, simplicity, diversity, and conduciveness to scale-up of the technique far outweigh any of its drawbacks. For this reason, the focus of this review will be on the use of electrospinning to produce nanofibrous tissue engineering scaffolds.

3. Characteristics of tissue engineered nanofibrous structures

The appeal of nanofibers in tissue engineering is their structural similarity to native ECM; however, ECM not only has a structural role but also a functional one. This network creates a dynamic, three-dimensional microenvironment in which cells are maintained. Signals are transmitted between the cell nucleus and the ECM enabling communication between both for cell adhesion, migration, growth, differentiation, programmed cell death, modulation of cytokine and growth factor activity, and activation of intracellular signaling [19,27]. In addition, the interactions between cell receptors and ECM molecules are critical for wound healing and development of nature's provisional matrix for cellular migration, proliferation, and subsequent tissue remodeling. The influence of the ECM on cellular activities occurs via binding of specific factors to specific ECM molecules and binding of ECM molecules to cell surface receptors known as integrins, which then influence local release of growth factors or separation of molecules (for cell attachment, spreading, and growth) [28,29].

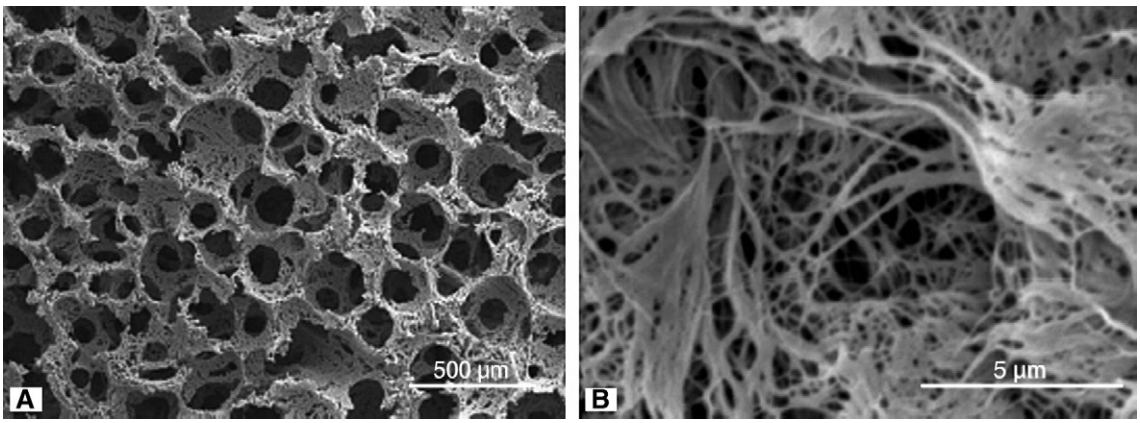

Fig. 2. Scanning electron micrographs of a nanofibrous PLLA matrix that was created through phase separation with paraffin spheres 250–420 μm in diameter, and has a porosity of more than 97%. Reprinted from [15], copyright 2004, with permission from Elsevier.

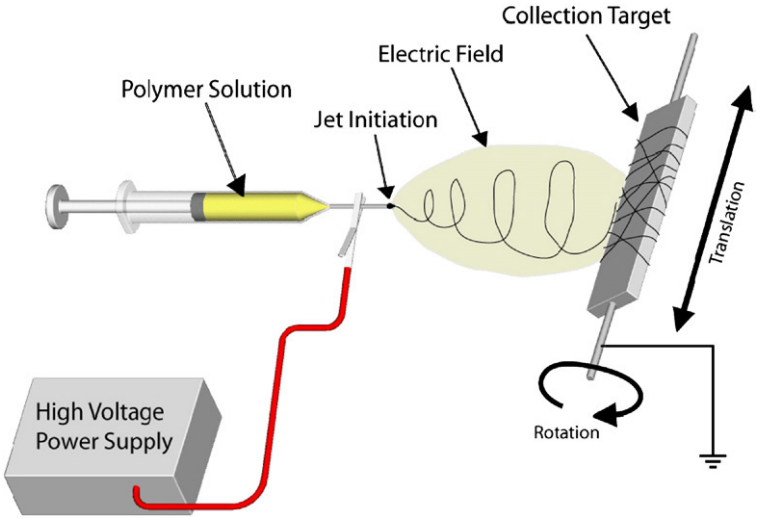

Fig. 3. A schematic of the electrospinning process to illustrate the basic phenomena and process components.

Beginning as soluble components processed within the cells, the ECM is secreted from the cells and is highly regulated by and specific to each tissue type and developmental stage [30]. ECM is composed of collagens, elastin, hyaluronic acid, proteoglycans, glycosaminoglycans, fibronectin, laminins, and molecules such as growth factors, cytokines, and enzymes and their inhibitors. It is known that cell–collagen interactions influence cell growth and differentiation depending on how well the cells are able to penetrate the interwoven fibrillar collagen ECM [19,31].

Current nanolevel processing techniques have been developed with the goal of mimicking ECM geometry. All three of the aforementioned techniques are capable of producing fibers with sub-micron diameters. Efforts have also been made to go beyond geometry and attempt to truly mimic the ECM in terms of physiological ability. By engineering material properties of synthetic polymer structures and surfaces, they can be made more conducive to cell adhesion and function. On the other hand, natural polymers may already contain/present signaling capabilities required by cells. Thus, materials utilized as nanofibers in tissue engineering include a variety of synthetic and natural polymers that offer advantages and disadvantages. There have been investigations into the use of xenogeneic and allogeneic ECM as tissue engineering devices [32,33]; but the problems associated with this approach include age-related factors, cell lysis, and calcification. The polymers electrospun in our lab offer the advantages of being readily available and having known degradation times and mechanical strengths [20]. However, these synthetic polymers lack an ultrastructure that mimics ECM; thus, we are also electrospinning natural polymers, *i.e.*, native ECM proteins, as previously mentioned, for tissue engineering applications. Yet even natural polymers have some disadvantages, including immunogenicity and variations in mechanical properties, degradation, and reproducibility [10].

4. Electrospinning of synthetic and natural polymers

4.1. Poly(glycolic acid)

PGA is a biodegradable aliphatic polyester used in a variety of medical applications. Initially developed as a suture for clinical

Table 1
Assessment of nanofiber processing techniques (adapted from [8])

Process	Lab/industrial application	Ease of processing	Advantages	Limitations
Self-assembly	Lab	Difficult	• Achieves fiber diameters on lowest ECM scale (5–8 nm)	• Only short fibers can be created (<1 μm) • Low yield • Matrix directly fabricated • Limited to a few polymers
Phase separation	Lab	Easy	• Tailorable mechanical properties, pore size, and interconnectivity • Batch-to-batch consistency	• Low yield • Matrix directly fabricated • Limited to a few polymers
Electrospinning	Lab/industrial	Easy	• Cost effective • Long continuous nanofibers • Production of aligned nanofibers • Tailorable mechanical properties, size, shape • Plethora of polymers may be used	• Large nanometer to micron scale fibers • Use of organic solvents • No control over 3D pore structure

use in the 1970s, PGA was found to have better than average tissue compatibility and reproducible mechanical properties such as strength, elongation, and knot retention. Some characteristics of the polymer include a moderate crystallinity (46%–52%), a high melting point (225 °C), and low solubility in organic solvents [34,35]. An advantage of PGA is its predictable bioabsorption; the *in vivo* degradation rate of PGA monofilaments ranges from 2 to 4 weeks due to its hydrophilic nature [34,36]. Hydrolytic degradation accounts for the nearly 60% loss of strength during the first 2 weeks and is characterized by sharp decreases in local pH and crystallinity [37]. It should be noted that the glass transition temperature of PGA is close to physiologic temperature. At and above this temperature, water diffusion and hence hydrolysis are more easily accomplished [34].

Traditional extrusion methods result in PGA fibers with minimum diameters above 10 μm [38]. This limitation has been overcome with the use of electrospinning. PGA has been successfully electrospun into matrices with sub-micron fiber diameters and known degradation times for tissue engineering applications by Boland et al. [5,39,40] and You et al. [41].

Our laboratory has produced electrospun mats of PGA in 1,1,1,3,3,3-hexafluoro-2-propanol (HFP) composed of fibers with diameters ranging from approximately 1.5 μm to less than 200 nm [5,39,40]. Control over fiber diameter has been accomplished by utilizing various polymer to solvent concentrations (weight to volume ratios), as illustrated in Fig. 4.

The mechanical properties of the scaffolds, including tangential modulus and stress and strain to failure, can be tailored by controlling the geometry and orientation of the fibers in the scaffolds. The authors have evaluated the mechanical properties of the different PGA electrospinning concentrations in both aligned and random fiber orientation scaffolds [40]. Fig. 5 summarizes the results of this study in terms of the elastic modulus and strain at failure of PGA in a uniaxial model. The overall results exhibit a correlation between the fiber diameter and orientation and the elastic modulus and strain to failure. Additionally, it has been shown that the greater surface area to volume ratio of smaller fibers results in a faster loss of strength during degradation. When an initially tough (high strength and elasticity) and fast degrading material is desired, PGA is a good choice. However, the higher rate of degradation may result in sharp increases in localized pH which may cause unwanted tissue responses if the region does not have a high buffering capacity or sufficient mechanisms for the rapid removal of metabolic waste [34]. Biocompatibility studies have been performed by the authors, in which PGA and acid treated PGA were evaluated in cell culture and in an animal model [5]. Both fiber diameter and acid pretreatment influenced the *in vitro* and *in vivo* cellular responses. The acid pretreatment improved biocompatibility via a hypothesized mechanism of surface hydrolysis of ester bonds, thereby exposing carboxylic acid and alcohol groups [39]. This may improve vitronectin binding which, in turn, may improve the ability of cells to adhere to the surface.

4.2. Poly(lactic acid)

PLA is another biodegradable aliphatic polyester that is very popular for use in medical applications [34]. Our lab uses PLA synthesized from the more common L optical isomer (sometimes denoted PLLA) instead of the D or *dl* isomers, since L-lactic acid,

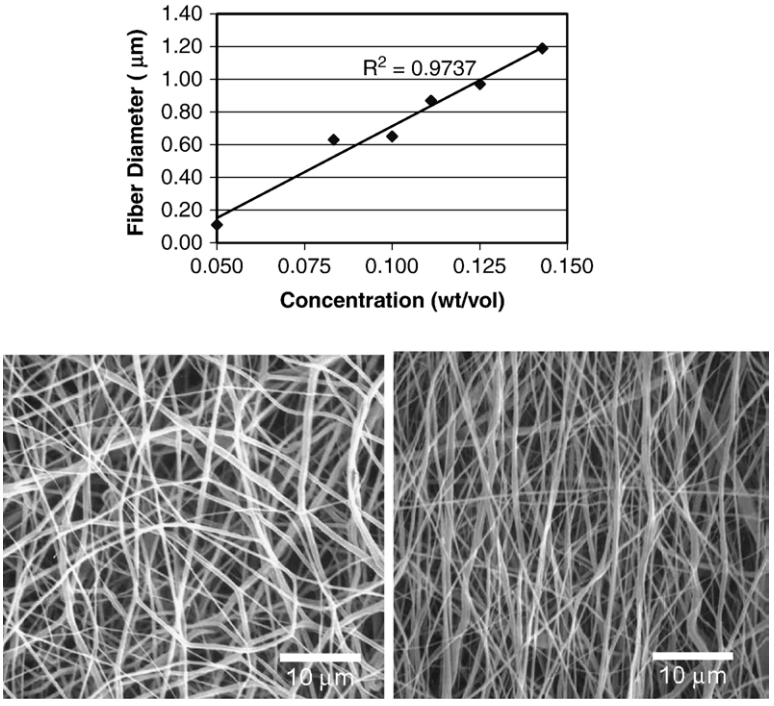

Fig. 4. (Top) Graph demonstrating the linear relationship between fiber diameter and initial concentration of PGA in HFP; fibers ranging from less than 200 nm to over 1.2 μm were produced. (Bottom) SEMs of electrospun PGA (0.143 g/ml in HFP) showing the random fiber arrangement (left) and the aligned fiber orientation (right) (1600× magnification). Reprinted with permission from [40]. Copyright 2001 Taylor and Francis Group.

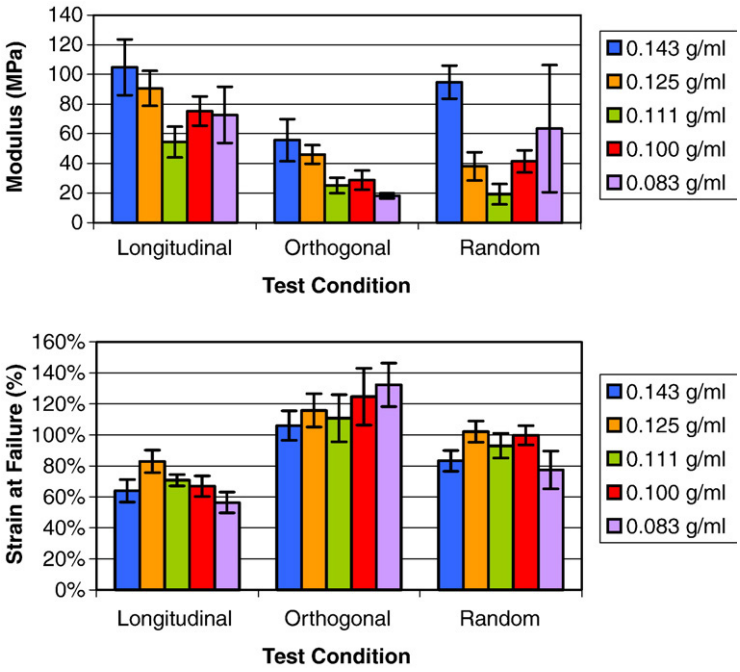

Fig. 5. (Top) Modulus of elasticity and (Bottom) strain at failure measurements presented as a function of test condition, *i.e.*, in an aligned mat (tested longitudinal and orthogonal to the axes of the aligned fibers) and in a random mat, for varying concentrations (g/ml) of PGA in HFP. Reprinted with permission from [40]. Copyright 2001 Taylor and Francis Group.

the product of PLA hydrolysis, occurs naturally in the metabolic pathway in humans. The methyl group in the monomer makes PLA more hydrophobic than PGA; it also presents a steric hindrance that gives PLA a higher solubility in organic solvents and significantly slows hydrolysis such that PLA typically degrades within 30 to 50 weeks [35,36]. PLA also has a moderate crystallinity (about 37%) but has a lower melting point (96 °C) than PGA [34,36].

Like PGA, PLA can be processed with traditional fiber extrusion methods such as in biodegradable sutures, but resulting fiber diameters are on the micro-scale. Our laboratory has electrospun PLA in chloroform, methylene chloride, and HFP at concentrations ranging from 1/7 to 1/10 weight/volume ratios, resulting in fiber diameters ranging from 100 nm to about 10 μm depending on solvent and concentration (Fig. 6). Uniaxial tensile testing of these PLA electrospun mats revealed moduli on the order of 180 MPa. Nanoscale fibers of PLA have attracted the interest of numerous researchers. PLA has been electrospun by Yang et al. to produce aligned scaffolds for the study of neurite outgrowth and differentiation of neural stem cells seeded onto the scaffolds [42]. Other groups have utilized electrospun PLA scaffolds to investigate morphology and biodegradation rates [41,43], which could be used for such applications as drug delivery [44].

4.3. Poly(glycolic acid) and poly(lactic acid) blends and copolymers

When a single polymer does not have the properties desired for a tissue engineering application, a copolymer or blend (simple mixture) of polymers may be employed to achieve the desired geometrical, mechanical, and biodegradation properties. Electrospinning again allows the ability to produce nanofibers of such a copolymer or blend. Our laboratory has tested copolymers of poly (lactide-*co*-glycolide) (PLGA), at ratios of 75%PLA–25%PGA and 50%PLA–50%PGA, and we have blended PLA and PGA together in HFP at ratios of 100:0, 75:25, 50:50, 25:75, and 0:100 PLA:PGA. Preliminary data of such blends (prepared at a constant solid to solvent concentration of 0.143 g/ml for each polymer) showed that the fiber diameters ranged from 900 nm to 1.3 μm for aligned fibrous scaffolds and from 1.0 to 1.3 μm for randomly oriented fibrous scaffolds with no significant differences among any of the fiber dimensions produced irrespective of the blend ratio [35,45]. However, we have found that the fiber diameters of the copolymeric and blended scaffolds appear to be comparable to fiber dimensions of PGA alone at varying polymer concentrations. This could be a function of the reduced solubility of PGA dictating surface tension and thereby affecting the formation of the Taylor cone. From our experience, mechanical properties, such as tangential modulus, peak stress, and strain to failure, of scaffolds made from these copolymers and blends do appear to be controlled by the fiber/polymer composition. Preliminary mechanical testing data on the blends mentioned above is given in Fig. 7. Further experimentation, utilizing such techniques as nuclear magnetic resonance (NMR) spectroscopy, could elucidate the differences in fiber makeup [46].

Properties of electrospun PLGA including degradation rate, hydrophobicity, and crystallinity have been investigated thoroughly by several groups [41,47,48]. PLGA was electrospun into nanofibrous structures, with fibers ranging from 500 to 800 nm in diameter, for analysis as scaffolds for soft tissues such as cartilage and skin [49]. Other applications of electrospun PLGA include

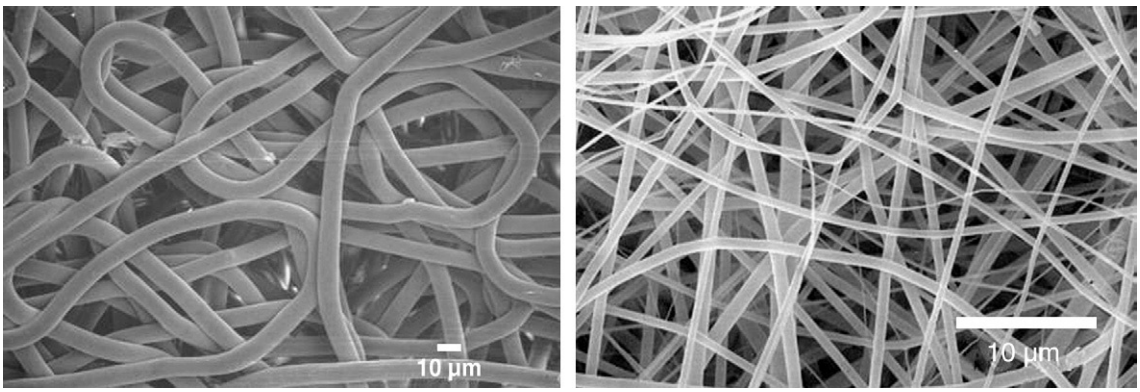

Fig. 6. (Left) Scanning electron micrograph of randomly oriented PLA electrospun from chloroform; 10.3±1.3 μm mean fiber diameter (400× magnification). (Right) Scanning electron micrograph of randomly oriented PLA electrospun from HFP; 780±300 nm mean fiber diameter (2000× magnification).

cardiac tissue regeneration [50], in which scaffold effects on cardiomyocyte attachment, structure, and function were studied, and drug delivery, in which release of antibiotics during wound healing was studied [51].

4.4. Polydioxanone

PDO is a highly crystalline (55% crystalline fraction), biodegradable polyester that was originally developed for use as

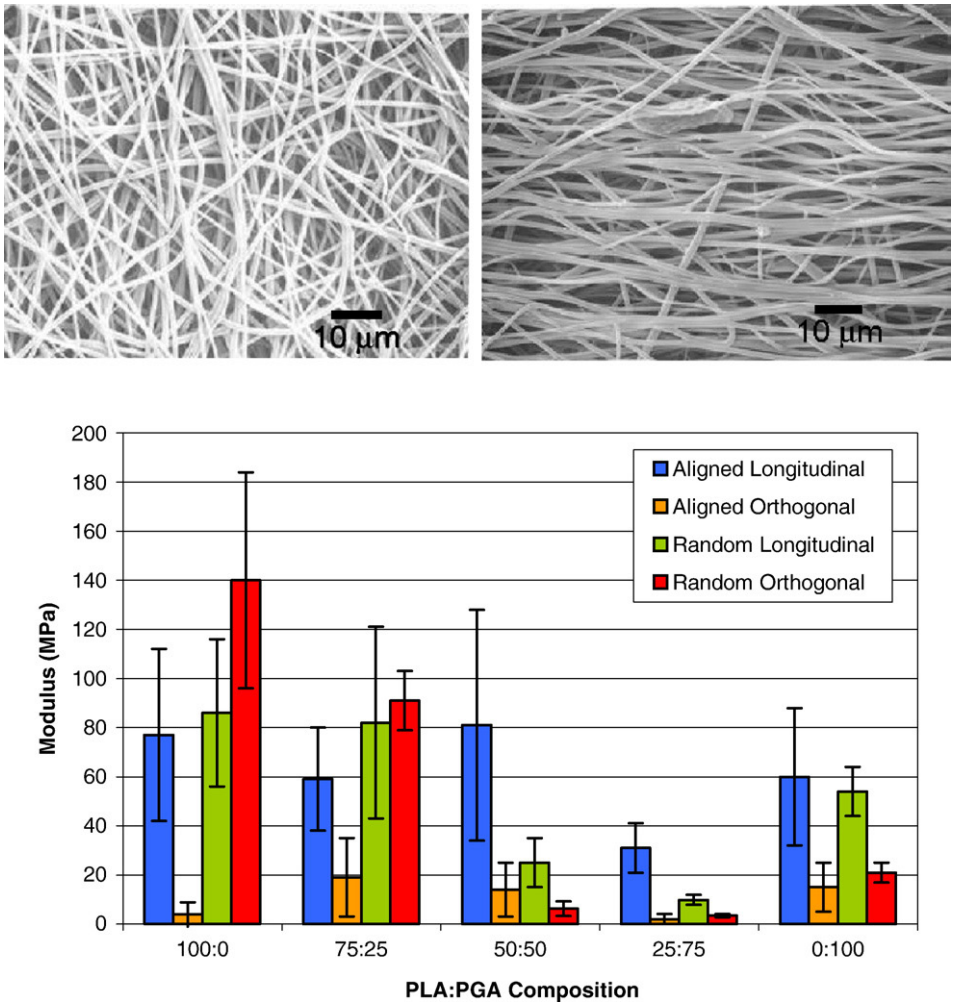

Fig. 7. (Top) Scanning electron micrographs of electrospun blends of (left) randomly oriented 75:25 PLA:PGA (1000× magnification) and (right) aligned 75:25 PLA:PGA (1000× magnification). (Bottom) Modulus as a function of polymer content in the blend for aligned and randomly oriented scaffolds based on direction of testing (longitudinal/orthogonal to primary fiber direction) [45].

a degradable suture (Ethicon, Inc., a Johnson and Johnson Company). The lifespan of PDO sutures within the body falls between the degradation rates of PGA and PLA, and was therefore thought to be an excellent suturing material. PDO also exhibits excellent flexibility due to the incorporation of an ester oxygen in the monomer backbone. However, there are several negative aspects of PDO as a suturing material that have come to light through the loosening of fine surgical knots. This loosening occurs for two reasons: PDO has shape memory that causes the suture to retain its spooled shape and the sutures themselves have a very low amount of surface friction, which when coupled with the material's shape memory can make knot retention very difficult. However, the same traits that prevent PDO from being an ideal suturing material may allow it to become a valuable material for the creation of tissue engineered scaffolds. The shape memory of PDO may actually provide rebound and kink resistance if formed into a vascular conduit. This unique trait coupled with the material's excellent biocompatibility, strength, and elasticity may prove beneficial to the creation of future engineered vascular grafts [35,52].

PDO has proven to be readily dissolvable in HFP, and has been successfully electrospun at concentrations between 42 and 167 mg/ml, producing fibers that ranged linearly from 180 nm to 1.4 μm, respectively (Fig. 8). Uniaxial tensile testing has been performed on various electrospun PDO concentrations in both aligned and randomly oriented scaffolds to determine the material's mechanical characteristics. This revealed a modulus ranging from 2.0 to 46 MPa, a peak stress ranging from 1.7 to 12.0 MPa, and a percent strain at break ranging from 31 to 240% [35,52]. These mechanical properties can be compared to two of the major structural components in soft tissues, collagen and elastin [53]. Collagen displays the following properties: modulus ranging from 100 to 2900 MPa, peak stress ranging from 5 to 500 MPa, and percent strain at break ranging from 5 to 50%. Elastin exhibits a modulus ranging from 0.3 to 0.6 MPa, a peak stress ranging from 0.36 to 4.4 MPa, and a percent strain at break ranging from 100 to 200%. The modulus achieved for the electrospun PDO specimens falls between the maximum modulus of elastin and the minimum modulus of collagen. Peak stress exhibited by the electrospun PDO is within the range of elastin and near the lower limit of collagen. The percent strain at break range of electrospun PDO spans both the ranges of elastin and collagen, and even exceeds the upper limit of collagen. This data shows that from a mechanical standpoint the bulk material properties of electrospun PDO are on the same order of magnitude as the major structural components of the native vascular ECM.

4.5. Polycaprolactone

PCL is a relatively inexpensive, highly elastic polyester that demonstrates a lack of toxicity and a slow degradation time (1–2 years) [34,54,55]. The ability to electrospin pure PCL was published by Reneker as a solution in acetone at 14 to 18 wt.%. PCL fibers were shown to contact and merge within the electrospinning jet to form garland-like fibrous structures [56]. Yoshimoto et al. electrospun PCL at 10 wt.% from chloroform for a bone tissue engineering application [54], and Shin et al. electrospun PCL from a 1:1 mixture of chloroform and methanol to form a tissue engineered cardiac graft [57]. In both of the previous tissue engineering applications, PCL was chosen for its good mechanical properties (modulus and elasticity) and slow degradation rate. After pre-coating with soluble collagen, the material was also found to exhibit acceptable cellular interaction. Fujihara et al. electrospun PCL scaffolds at 3 to 7.5 wt.% from a chloroform/methanol solution (75:25 wt.%) that contained calcium carbonate nano-particles (PCL:$CaCO_3$ 75:25 and 25:75 wt.%) for use as a guided bone regeneration membrane. These membranes were composed of nanoscale fibers and were capable of sustaining good osteoblast attachment and proliferation for the duration of their trials [58]. Li et al. were able to successfully electrospin nanofibrous PCL scaffolds at 0.14 g/ml from a 1:1 mixture of tetrahydrofuran and *N*, *N*, dimethylformamide. Human mesenchymal stem cells (hMSCs) were seeded on these scaffolds and induced to differentiate along adipogenic, chondrogenic, and osteogenic lineages using specific differentiation media to demonstrate the potential of PCL as a scaffolding material for cell based, multiphasic tissue engineering [59].

4.6. Poly(glycolic acid) and polycaprolactone blends

As one would expect, the addition of the highly elastic PCL to PGA leads to an increase in the extensibility of the electrospun blend matrix. Electrospinning of the blends appears to be limited to 1/3 PCL by weight in HFP. Experimentally, we have seen strain to failure in excess of 400% for these scaffolds. Like the PGA–PLA blends, we do not see a wide variance in fiber diameters and must assume that the individual polymers become entangled in a regular pattern dictated by their chemistry and concentration. This blend seems well suited to tissue engineering applications where high elasticity is the driving factor. In addition, due to the long degradation time of PCL (typically 1–2 years), it would be reasonable to expect that the blend would degrade slower than PGA alone. Support for this prediction comes from the work of Barralet et al. While they did not use electrospun blends of PGA and PCL, they did determine that PGA fiber meshes that had been stabilized by dip coating in PCL were able to maintain their structure in culture (using human biliary epithelial cells) for at least three months, while unstabilized PGA scaffolds degraded within 28 days [60]. This increased degradation time due to the presence of PCL should also be evident in the electrospun blends of the two polymers, in which the polymers' chains would be intertwined, affording the PGA some shielding from hydrolysis much like a dip coating procedure.

4.7. Poly(lactic acid) and polycaprolactone blends

PLA:PCL blends and copolymers have been proven to possess great solvent flexibility, much like pure PLA, as they can be electrospun from either chloroform or methylene chloride. They also exhibit a percent increase in elasticity that is even more pronounced than with PGA:PCL blends, while maintaining an ultimate tensile strength that is analogous to that found for pure PLA scaffolds. By adding a small amount of PCL (as little as 5 wt.%) to PLA, the strain to failure of a scaffold increased from less than 25%

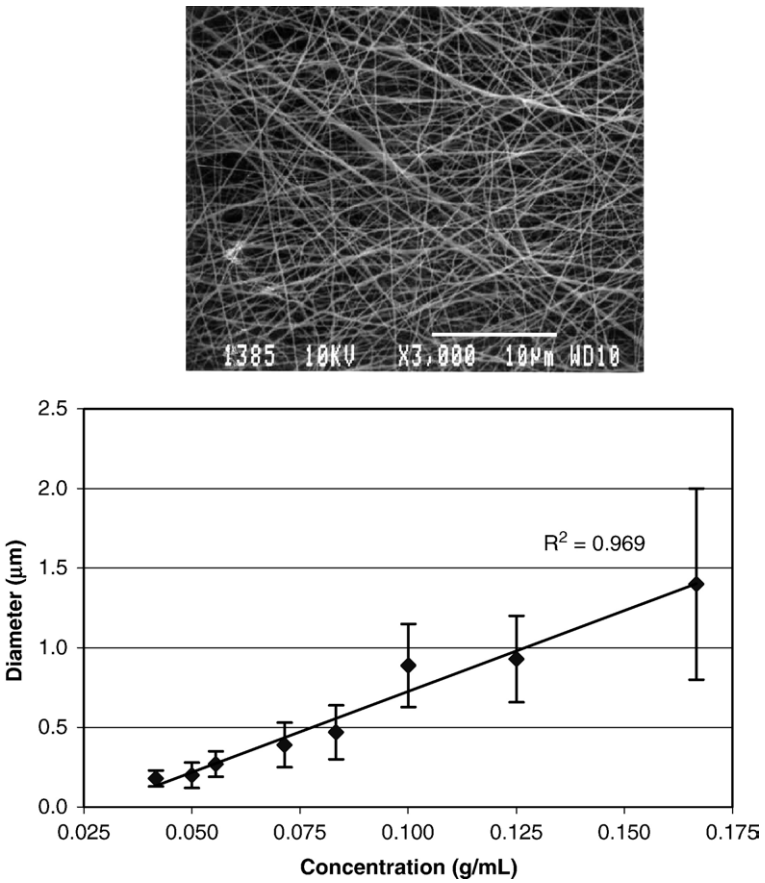

Fig. 8. (Top) Scanning electron micrograph of 180 nm diameter randomly oriented fibrous structures produced from 42 mg/ml PDO in HFP (3000× magnification). (Bottom) Results of the fiber diameter analysis versus PDO concentration illustrating the linear relationship between electrospinning solution concentration and fiber diameter. Reprinted with permission from [52]. Copyright 2005 Elsevier.

to more than 200%. Typical strain to failure values that our lab has determined for these PLA:PCL blends are illustrated in Fig. 9. Other labs have tried electrospinning copolymers that contain larger amounts of PCL. Kwon et al. successfully electrospun poly(L-lactide-*co*-ε-caprolactone) (PLCL) at various weight percents from methylene chloride in ratios of 70:30 (9 wt.%), 50:50 (7 wt.%), and 30:70 (11 wt.%). At 25 °C the 70:30 ratio was a hard solid, the 50:50 ratio was an elastomer, while the 30:70 ratio was a gummy solid that upon further investigation was found not to consist of fibers, but a fused mesh. The two ratios that resulted in fibrous scaffolds, 70:30 and 50:50, were determined to have a Young's modulus of 14.2 and 0.8 MPa, respectively [61].

With a tensile strength comparable to that of PLA and the added elasticity provided by the addition of PCL, these combinations show a great deal of promise for use as an arterial graft. An engineered vascular graft must be strong enough to accommodate a large pressure increase while having enough elasticity to passively expand to accept a large bolus of blood and

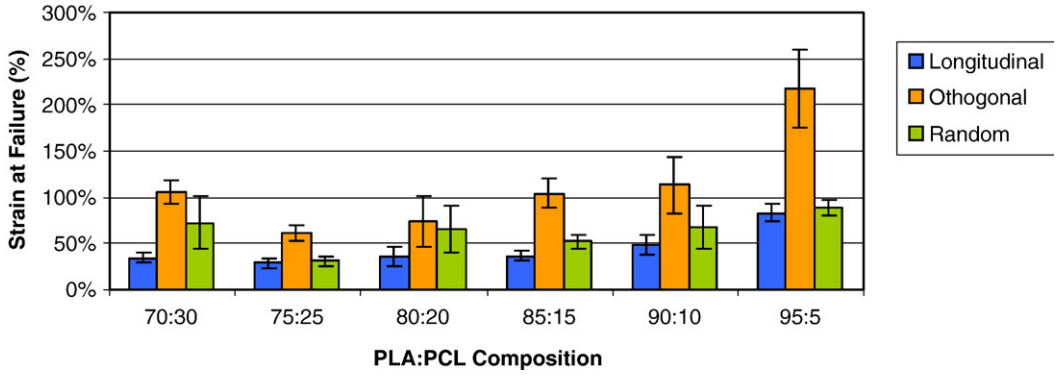

Fig. 9. This figure illustrates that the strain to failure of a tissue matrix is a function of both composition (varying blend ratios of PLA and PCL) and fiber alignment (longitudinal/orthogonal to primary fiber direction).

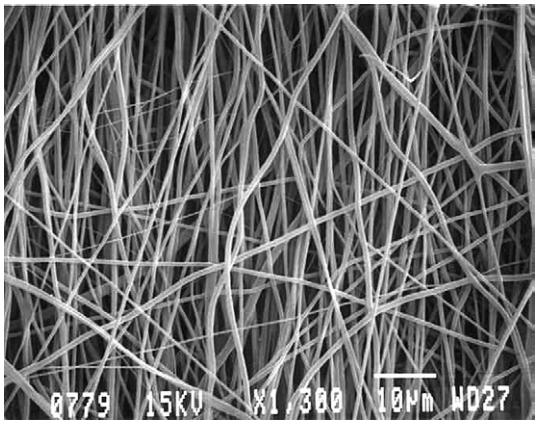

Fig. 10. Scanning electron micrograph illustrating aligned fibers composed of an 85:15 PLA:PCL blend from a 0.143 g/ml solution in HFP.

contract to push the blood downstream. In addition, this graft should be composed of highly aligned nanofibers to add radial and longitudinal strength to the construct. The scanning electron micrograph in Fig. 10 typifies the capacity to align fibers during electrospinning.

Building upon previous work on electrospun PLA vascular grafts by Stitzel et al. [46], Xu et al. electrospun a nanofibrous mat of P(LLA-CL) (75:25). This scaffold was composed of 550± 120 nm fibers and exhibited a tensile modulus of 156 MPa, tensile strength of 5 MPa, and strain at break of 127%. This compares favorably to the mechanical properties of native coronary artery having a tensile strength of 1.40–11.14 MPa and a strain at break of 45–99%. Furthermore, smooth muscle and endothelial cells were seeded on these scaffolds and cultured for 7 days with favorable results [62].

4.8. Polydioxanone and polycaprolactone blends

As with other moderately crystalline polyesters (*e.g.*, PGA, PLA), the addition of PCL to electrospun PDO scaffolds was expected to increase the ultimate strain at break, while having a minimal effect on both the average fiber diameter and peak stress. Our lab electrospun various concentrations of PCL (233 mg/ml, 500 mg/ml) blended with PDO (100 mg/ml) from HFP in several different PDO:PCL ratios (100:0, 90:10, 70:30) (unpublished data). This produced fibers that ranged from 940 nm for pure 100 mg/ml PDO to 1.5 µm for the 70:30 ratio of 100 mg/ml PDO:500 mg/ml PCL (Fig. 11).

Uniaxial tensile testing after a 24-h soak in phosphate buffered saline at 37 °C revealed that electrospun PDO:PCL blends do not behave in the same way as the two previous polyester copolymers do. While PGA:PCL and PLA:PCL resulted in ultimate strains that were markedly increased over pure PGA and pure PLA, the PDO:PCL blends actually experienced an ultimate strain that was less than that of pure PDO (Fig. 12). Neither the peak stress nor the fiber diameters were adversely affected. The cause of this reduced ultimate strain will be further investigated by our laboratory.

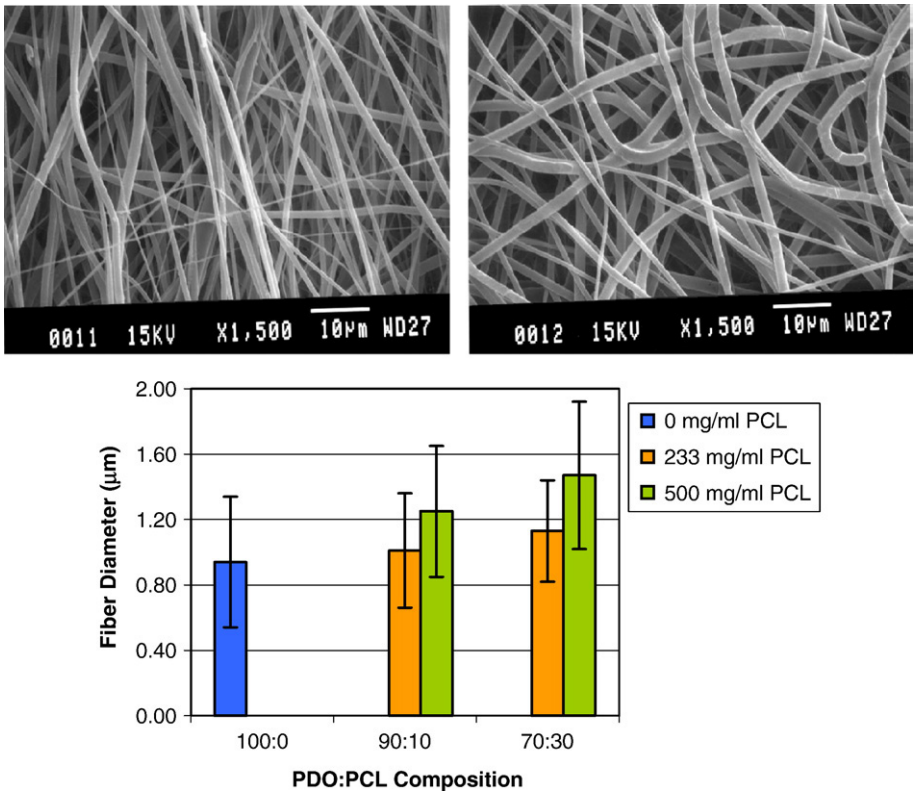

Fig. 11. (Top) Scanning electron micrographs of 100 mg/ml PDO:500 mg/ml PCL blends at ratios of 90:10 (left) and 70:30 (right). (Bottom) Results of fiber diameter versus PDO:PCL ratio for varying concentrations of PCL (mg/ml), illustrating the minimal difference in fiber size seen with inclusion of PCL to a PDO electrospun scaffold.

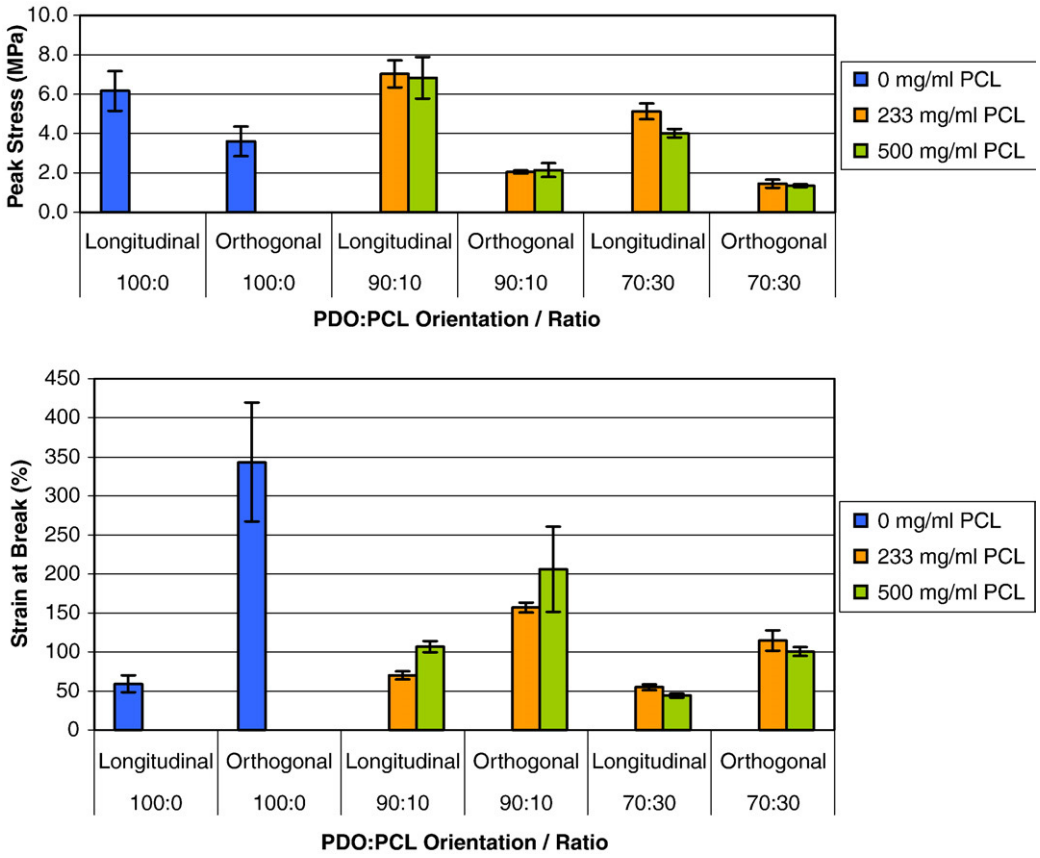

Fig. 12. (Top) Peak stress values for various PCL concentrations versus PDO:PCL ratio and orientation of the testing specimen (Longitudinal/Orthogonal to the principal fiber direction). (Bottom) Strain at break values for various PCL concentrations versus PDO:PCL ratio and orientation of the testing specimen.

4.9. Elastin

Elastin is the most linearly elastic biosolid known. It is a highly insoluble, hydrophobic protein that the body utilizes extensively in organs where shape and energy recovery are critical parameters. It constitutes a large proportion of the walls of arteries and veins to provide elastic recoil and to prevent the dissipation of transmitted pulsatile energy into heat. It is also a large component of ligaments and lung parenchyma due to its elastic properties. The skin contains thin strands of elastin that help to keep it taught and smooth [63,64]. Such a diverse and essential protein could prove to be extremely effective as a tissue scaffold or graft, particularly in vascular applications. Huang et al. were able to electrospin a synthetically based elastin-mimetic. This synthetic elastin was created out of an 81 kDa recombinant protein that was based on the repeating elastomeric peptide sequence of elastin, and was able to produce fibers that were between 300 and 400 nm in diameter [63]. Our lab successfully electrospun solubilized elastin (bovine neck ligament) at concentrations ranging from 200 mg/ml to 333 mg/ml in HFP, which resulted in the creation of a scaffold of flat, ribbon-like fibers. As these fibers were in fact ribbon shaped and not cylindrical, there was no true diameter. Therefore, the breadth of these fibers was determined, and found to range from 2.09 to 3.36 μm across. As has been the norm with electrospun polymers, where an increase of polymer concentration leads to a linear increase in fiber diameter, the breadth of the electrospun elastin fibers increased linearly with concentration (Fig. 13).

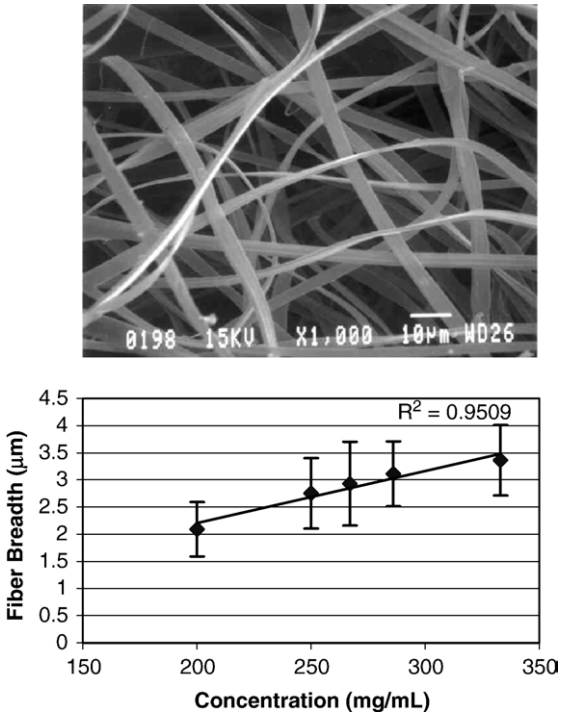

Fig. 13. (Top) Scanning electron micrograph of electrospun elastin scaffold at 250 mg/ml. (Bottom) Results of fiber dimension analysis versus electrospun elastin concentrations illustrating linear relationship between fiber size and concentration.

Through uniaxial testing, it was shown that the non-hydrated electrospun elastin scaffolds retained a good amount of elasticity, with the 200 mg/ml concentration achieving an ultimate strain of 206% (Fig. 14).

Our lab has recently electrospun blends of several different ratios of elastin and PDO (100:0–50:50 PDO:elastin by volume) to create bioactive scaffolds that remain mechanically viable [65]. Preliminary *in vitro* cell culture work showed elastin-containing grafts to be bioactive, with cells migrating through their full thickness within 7 days. In order to assess the mechanical properties of the blended scaffolds, we have performed uniaxial tensile and suture retention tests on the electrospun grafts, yielding results whose range includes the values of native vessel. We also electrospun 6 mm ID seamless tubes for the testing of graft compliance. Dynamic compliance measurements produced values that ranged from 1.2 to 5.6%/100 mmHg for a set of three different mean arterial pressures, with the 50:50 ratio closely mimicking the compliance of native femoral artery.

4.10. Collagens

4.10.1. Gelatin

Denatured collagen, or gelatin, is of interest in tissue engineering because of its biological origin, excellent biodegradability and biocompatibility, and commercial availability at low cost. It has been used for many years as a vascular prosthetic sealant, a carrier for drug delivery, and a dressing for wounds. Only recently, through electrospinning, has it gained interest as a tissue engineering scaffold. However, even as an electrospun nanofibrous scaffold, gelatin constructs must be fixed to prevent them from dissolving in water at temperatures 37 °C or above and congealing into gels at lower temperatures. Zhang et al. created electrospun matrices of gelatin in TFE at various weight to volume ratios to determine the optimal concentration of gelatin for electrospinning by way of fiber morphology observations. This revealed that gelatin performed best at 10% w/v, with a tensile strength of 2.5 MPa and an ultimate strain of 64% [66]. Li et al. electrospun gelatin in HFP to compare its cell attachment and migration characteristics to collagen, elastin, and recombinant human tropoelastin. They electrospun various concentrations of gelatin ranging from 2 to 8.3% w/v and obtained fiber diameters between 200 and 500 nm. Human embryonic palatal mesenchymal cells (HEPM) were seeded on each of the four scaffolds, and allowed to culture for 6 days. Gelatin behaved in much the same manner as the other proteins, in that it supported cell attachment, migration, and proliferation for the duration of the trial [67].

4.10.2. Fibril-forming collagens

The fibril-forming collagens, types I, II, and III, are the most abundant proteins (natural polymers) in the body, are found throughout the interstitial spaces, and provide the overall structural integrity and strength to tissues. More importantly, the collagen structure (ECM) provides the cells with the appropriate biological space for embryologic development, organogenesis, cell growth, and wound repair [31].

In many native tissues, polymers of type I collagen are the principal structural elements of the ECM [27,68]. The underlying alpha chains that form these natural polymers are arranged into a repeating motif that forms a coiled structure. At the ultrastructural level, this repeating motif exhibits a 67 nm interval that imparts a characteristic banding pattern to the collagen fibril. Historically, collagen has been used in a variety of tissue engineering applications because of its prevalence in native ECM and because it can be isolated from a variety of sources and is relatively non-immunogenic. However, the typical procedures used to isolate and reprocess this natural scaffolding into an engineered material may compromise many of its biological and structural properties.

Work in our laboratory on the electrospinning of collagen type I (acid soluble) indicates the capability of reproducibly fabricating nanostructured, collagen-based tissue engineering scaffolds that retain biological and structural properties [68]. The electrospun collagen solutions ranged in concentration from 0.03 to 0.10 g/ml of HFP resulting in mats/scaffolds composed of 100 nm to 5 μm diameter fibers (Fig. 15). Electrospun calfskin type I collagen has been analyzed with transmission electron microscopy to reveal the 67 nm banding that is characteristic of native collagen (Fig. 15). Hence, an electrospun collagen mat may be a truly biomimicking scaffold, since sub-micron diameter fibers possessing the natural collagen ultrastructure can be created.

The near frictionless cartilage that lines articulating joints is essential for energy absorption and load distribution to the bones. Degenerative changes in the composition and structure of this articular cartilage alter chondrocyte function and are linked to the development of osteoarthritis, which may result in an inability of

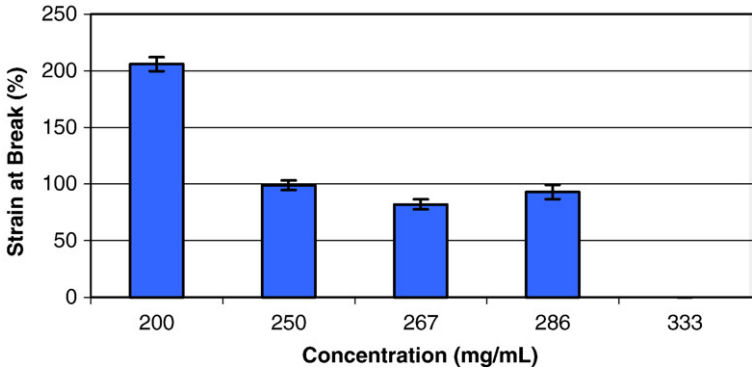

Fig. 14. Strain at break values versus electrospun elastin concentrations for dry samples that had been fixed in a 3% v/v glutaraldehyde vapor chamber for 10 min. We were unable to attain any data for the 333 mg/ml concentration.

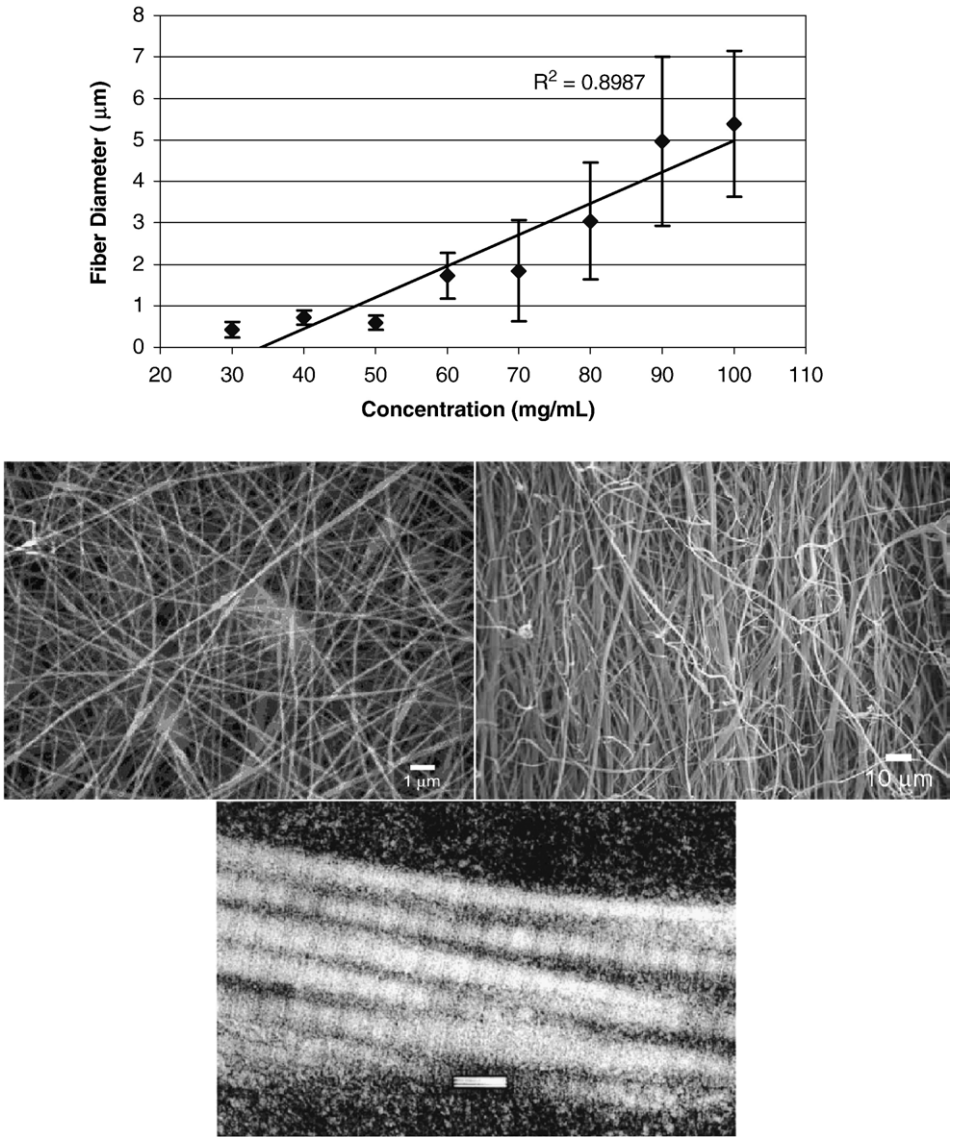

Fig. 15. (Top) Preliminary electrospinning data of calfskin collagen type I scaffolds from various collagen concentrations in HFP to demonstrate the linear relationship between fiber diameter and collagen concentration. (Middle) Scanning electron micrographs of electrospun calfskin collagen type I; the mandrel/target was rotated at a rate less than 500 rpm to produce randomly arranged mats (left — 4300× magnification) and at about 4500 rpm (an approximate velocity of 1.4 m/s at the mandrel surface) during electrospinning to allow for alignment of the collagen fibers (right — 430× magnification). (Bottom) Transmission electron micrograph cross-section of calfskin collagen type I fibers showing the traditional 67 nm banding of native collagen (scale bar=100 nm). Reprinted with permission from [68]. Copyright 2002 American Chemical Society.

mature cells to restore the damaged cartilage. Since the solid phase of the articular cartilaginous extracellular matrix is predominantly collagen type II, tissue engineered scaffolds of this macromolecule may enable the creation of tissue with both the function and morphology of native articular cartilage. Collagen type II has been electrospun for use in cartilage tissue engineering by Matthews et al. Electrospun chicken sternal cartilage collagen type II suspended in HFP at a concentration of 0.04 g/ml resulted in mats with fibers that averaged 110±90 nm in diameter [69]. Human articular chondrocytes seeded on the electrospun collagen type II scaffolds were shown to penetrate the thickness of the scaffold (by scanning electron microscopy and histological analysis). Electrospinning enables the construction of the structural zones of cartilage in which the nanofibrous collagen orientation and collagen and proteoglycan composition differ [69]. Shields et al. investigated differences in fiber diameter and mechanical properties of cross-linked (with glutaraldehyde vapors) and uncross-linked electrospun collagen type II scaffolds. Following 7 days of chondrocyte cell culture, scanning electron micrographs (SEMs) revealed cellular adherence to and infiltration of the scaffolds [6]. In a feasibility study (unpublished data), articular cartilage chips were removed from the joints of calves in different age groups and processed to extract collagen type II. The lyophilized collagen was dissolved in HFP at the concentrations of 0.06, 0.08, 0.10, and 0.12 g/ml; SEM analysis of fiber diameter and pore size revealed that a linear relationship existed between the concentration and both the pore size and fiber diameter as shown in Fig. 16, with mean fiber diameter and mean pore size

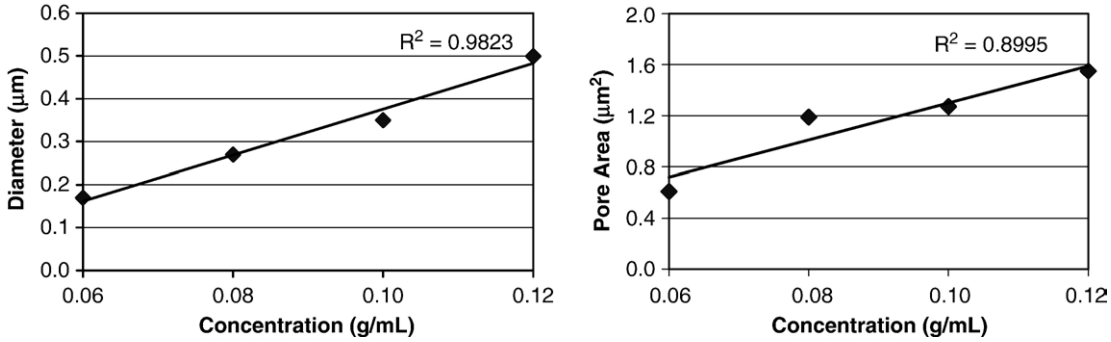

Fig. 16. Linear relationships between both mean fiber diameter and mean pore area and the concentration of collagen type II in HFP.

increasing as the concentration increased. Further work with electrospun collagen type II has been performed in our laboratory to analyze various cross-linking agents; use of carbodiimide in ethanol shows extreme promise in maintaining the structural integrity and enhancing the mechanical properties of the pure collagen fibrous scaffolds [70].

The feasibility of electrospinning collagen type III was performed in our laboratory with encouraging results. Fig. 17 shows an example of electrospun collagen type III (human placenta) dissolved in HFP; SEM analysis showed fiber dimensions of 250±150 nm and random fiber orientation within the mat. A relationship between electrospinning concentration and fiber diameters has also been determined to be linear (Fig. 17) [71].

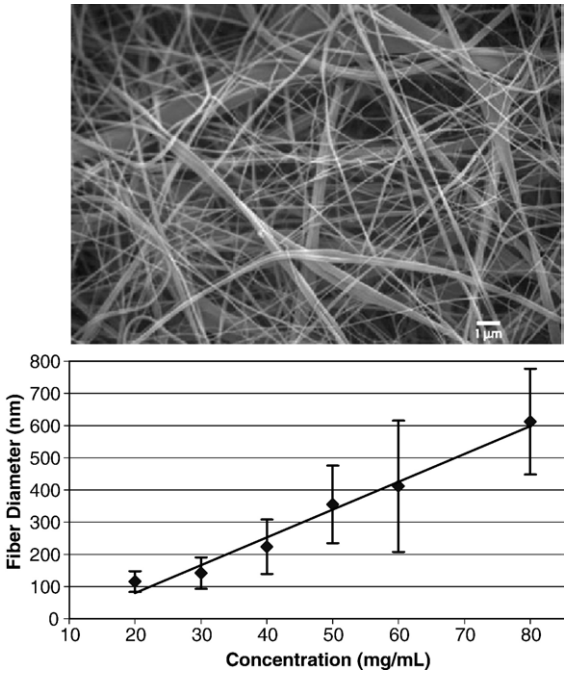

Fig. 17. (Top) Scanning electron micrograph of electrospun type III collagen (human placenta) in HFP depicting the random fiber orientation (4300× magnification) [72]. (Bottom) Linear relationship between collagen type III solution concentration and fiber diameter; the trendline shown has an R^2=0.981 [71].

4.10.3. Nonfibrillar collagens

The nonfibrillar collagens associate with the fibrillar collagens to form microfibrils and network structures (mesh-like structures). This group includes collagen type IV, which is a major structural element of all basal lamina and basement membranes. Preliminary data (unpublished) indicates that collagen type IV can be electrospun to form fibers ranging from 100 nm to 2 μm in diameter (Fig. 18), thereby adding the ability to incorporate additional functionality in terms of a tissue engineering scaffold during the electrospinning process.

4.10.4. Collagen blends

As is true with copolymers and blends of synthetic polymers, blending collagen with other natural and/or synthetic polymers will serve to enable further capability of tuning an engineering material to attain the desired properties. For example, Huang et al. have electrospun collagen type I and poly(ethylene oxide) to tailor fiber morphology and mechanical properties of scaffolds [4]. In our laboratory, the electrospinning of a blend of collagen types I and III from human placenta in a 50:50 ratio was investigated because types I and III collagen are often found together in many tissues including the blood vessel ECM [72]. Fig. 19 shows an electrospun blend of collagen type I and type III that were dissolved and mixed together/blended in HFP with the final combined collagen concentration at 0.062 g/ml; the measured

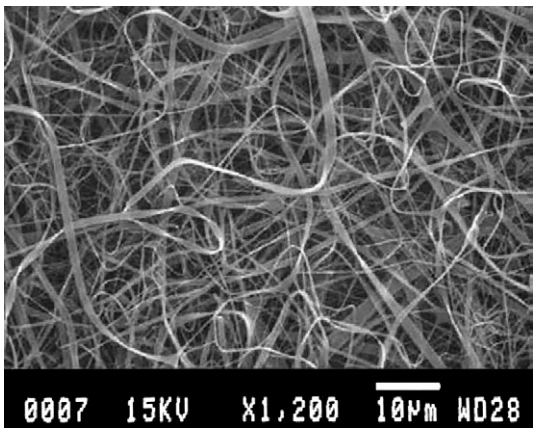

Fig. 18. Scanning electron micrograph of electrospun collagen type IV (125 mg/ml in HFP).

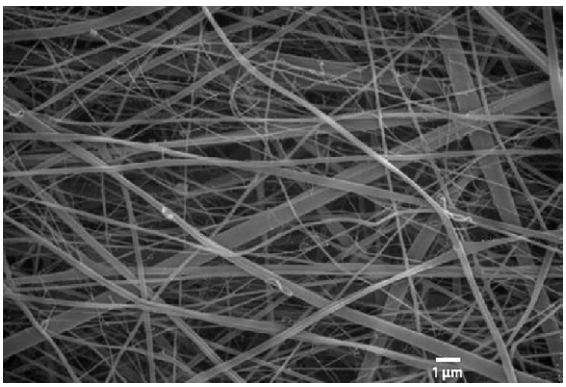

Fig. 19. Scanning electron micrograph of electrospun blend of type I and type III collagen (human placenta, 50:50) in HFP illustrating the random fiber orientation (4300× magnification) [72].

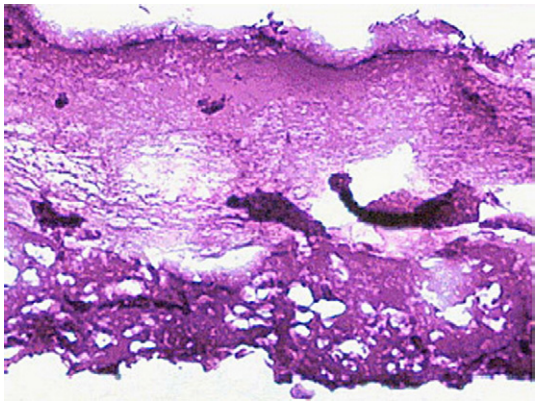

Fig. 21. Optical micrograph of electrospun collagen/elastin vascular graft depicting intimal, medial, and adventitial layers with complete cellular infiltration across the entire cross-section of the graft [72].

fiber diameter was 390±290 nm and the fibers were randomly oriented.

Native artery is comprised of three distinct layers: the intima, media, and adventitia. Each of these three layers has a different composition, making the creation of a biomimicking vascular graft extremely daunting. The intima is the innermost layer of native artery and is composed of a single layer of endothelial cells (ECs) on a basement membrane of collagen type IV and elastin. The media is the thickest layer of the artery, and is comprised of several layers of smooth muscle cells (SMCs) surrounded by an ECM of collagen types I and III, elastin, and proteoglycans. The adventitia is made of fibroblasts (FBs) and random ECM arrangements of collagen type I. Throughout all, elastin provides the artery with elastic recoil, while the collagens offer tensile strength. Having electrospun both elastin and collagen types I, III, and IV, our lab saw the opportunity to attempt the creation of a three-layered vascular construct (Fig. 20). An 80:20 collagen type I:elastin solution at a concentration of 0.083 g/ml was electrospun from HFP onto a 4 mm ID tubular mandrel, and subsequently seeded with both FBs and SMCs. Another tubular scaffold, this time 2 mm ID, was created with a 30:70 collagen type I:elastin solution. This electrospun scaffold was then inserted into the 4 mm ID scaffold, and the lumen filled with a SMC suspension. After 3 days in culture, a suspension of human umbilical vascular endothelial cells (HUVECs) was injected into the lumen, and the entire construct was cultured for two additional days. Histological examination revealed the scaffold to be a three-layered construct with complete cellular infiltration (Fig. 21). The artificial intima was covered by morphologically mature ECs, which resided upon a clearly defined basal lamina. SMCs were present throughout the media, and appeared to form a layer beneath the basal lamina where they had begun to align circumferentially around the axis of the scaffold. The FBs and SMCs in the adventitia created a dense population throughout the outermost wall. At the time of fixation, both the intimal ECs and the SMCs were actively proliferating [72]. As a feasibility study, Boland et al. constructed an electrospun fibrous scaffold from a blend of collagen types I and III (both human placenta collagen) and elastin (bovine ligamentum nuchae) (40:40:20) in HFP at a concentration of 0.083 g/ml; SEM analysis revealed random fiber orientation and a mean fiber diameter of 490±220 nm (Fig. 20) [72]. While much work remains on the creation of an ideal vascular graft, the beginning work here yielded promising results, and perhaps a step in the right direction.

The incorporation of glycosaminoglycans (GAG) into an ECM analogue during electrospinning could potentially be an important aspect in truly mimicking the native ECM. GAGs serve a variety of functions including linking collagen structures and binding growth factors. The specific GAGs of physiological and tissue engineering scaffold significance are hyaluronic acid, dermatan sulfate, chondroitin sulfate (most abundant GAG in tissues), heparin, heparan sulfate, and keratan sulfate. For example, an

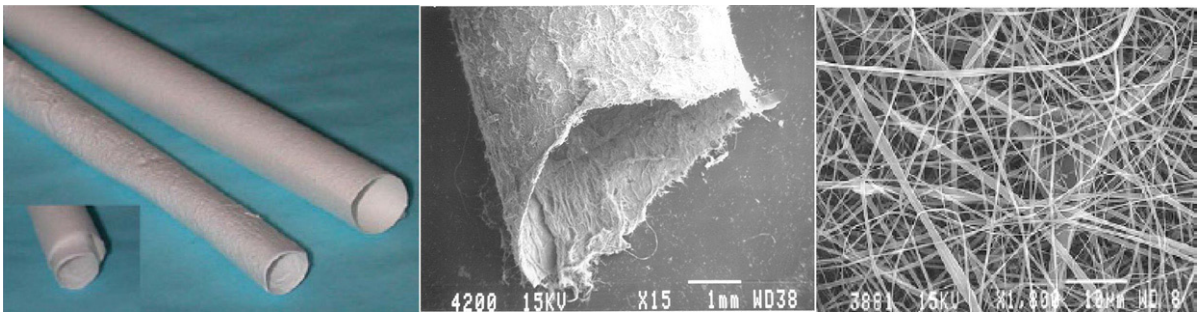

Fig. 20. (Left) Photograph of 2 and 4 mm ID electrospun scaffolds with an assembled composite structure. (Middle) Scanning electron micrograph of tubular electrospun composite. (Right) Scanning electron micrograph of electrospun 40:40:20 blend of collagen type I, collagen type III, and elastin that depicts randomly oriented fibers with an average diameter of 490±220 nm [72].

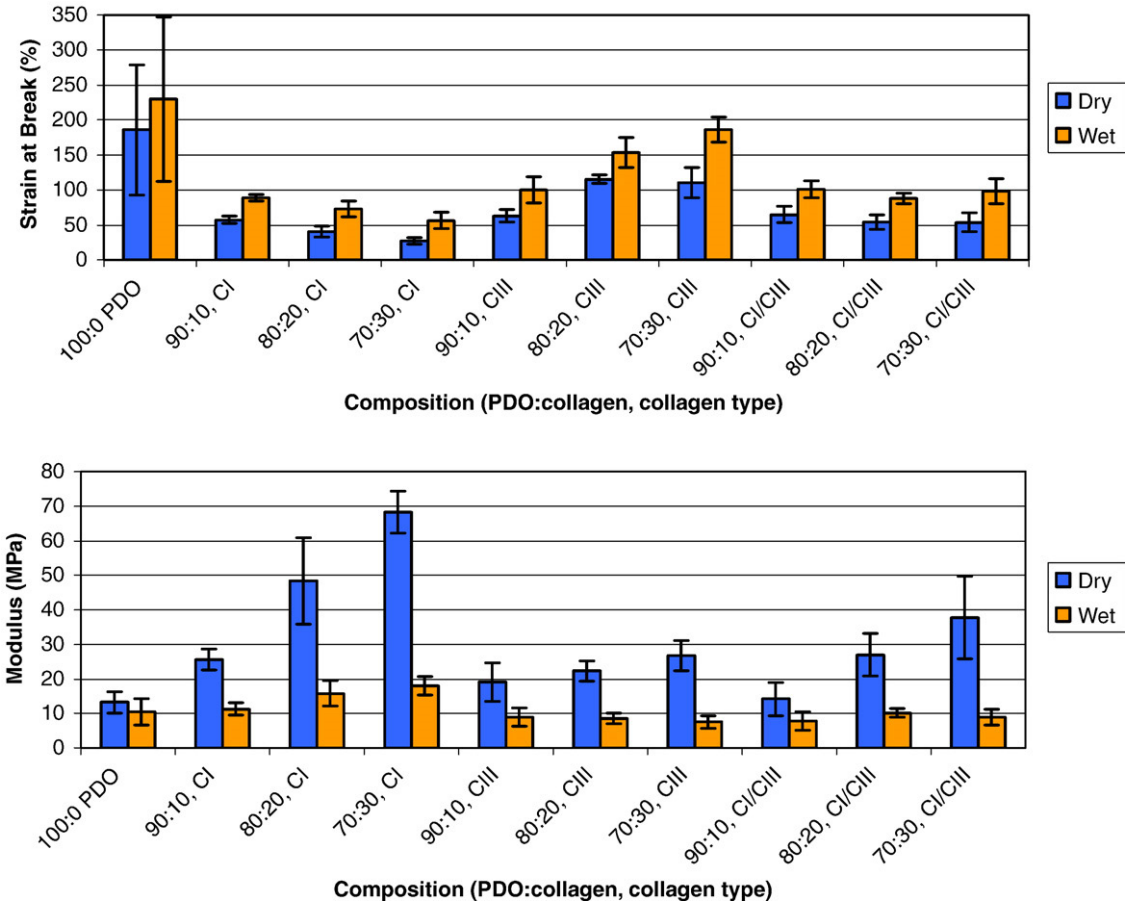

Fig. 22. (Top) Strain at break and (Bottom) tangential modulus presented as a function of the ratio of PDO to collagen type I (CI), collagen type III (CIII), or collagen types I and III (CI/CIII).

optimized collagen–GAG scaffold has been utilized extensively in dermal regeneration templates with unprecedented biological activity to enhance the healing response [73,74]. To date, our group has electrospun collagen–GAG blends by two methods (unpublished data): first, by adding the GAG directly to the electrospinning organic solvent (limited solubility) and, second, by dissolving the GAG at higher concentrations in distilled water prior to blending with the collagen/organic solvent. Preliminary results indicate that the dimensions of the fibers are decreased (relative to no GAG) due to the enhanced driving force brought about by the addition of the large charged molecules to the electrospinning solution. This result is not unexpected as a similar trend has been seen for the addition of organic salts to the electrospinning solution [75]. More specifically, this work has been performed by the addition of chondroitin sulfate to collagen type I for dermal regeneration templates and aggrecan (chondroitin sulfate/dermatan sulfate/keratan sulfate) to collagen type II for articular cartilage tissue engineering. In addition to this work with GAGs, Um et al. have published the results of electrospinning hyaluronic acid, to prepare non-woven nanofibrous structures [76].

One downside to any processed collagen structure is a lack of substantial strength upon hydration, which is true of electrospun collagen. Without substantial cross-linking of the electrospun

Table 2
Uniaxial mechanical properties (circumferential orientation) of e-PTFE [81], saphenous vein [82], and femoral artery [83,84]

Graft material	Elastic modulus (MPa)	Ultimate stress (MPa)	Strain at failure (%)
e-PTFE (30 μm internodal distance)	42–60	6–15	20–30
Saphenous vein	43	3	11
Femoral artery	9–12	1–2	63–76

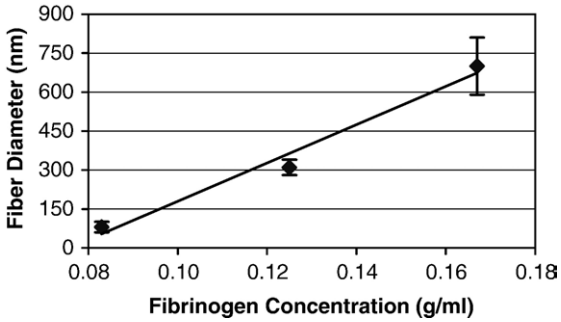

Fig. 23. Results of the electrospinning of various bovine fibrinogen concentrations in HFP/MEM with all other parameters constant to illustrate the linear relationship (R^2=0.98) between concentration and fiber diameter composing the structures produced. Reprinted with permission from [77]. Copyright 2003 American Chemical Society.

Table 3
Mechanical testing data for dry and hydrated electrospun fibrinogen (700 nm diameter random fibers)

	Dry structure	Hydrated structure
Elastic modulus (MPa)	84±41	0.3±0.05
Peak stress (MPa)	2.3±1.2	0.4±0.05
Strain at break (%)	8.3±3.7	134±18

collagen it does not have the strength to withstand arterial forces. However, extensive cross-linking with agents such as glutaraldehyde effectively turns the fibrous structure into leather with minimal bioactivity. Thus, our group has explored the electrospinning of the biodegradable synthetic polymers and their blends with collagen for structures requiring immediate strength such as an acellular vascular prosthetic. As an example, PDO was selected for this application due to its biocompatibility, degradation rate, and mechanical properties (high strength and shape memory).

In a preliminary study, we blended in solution collagen type I and type III with PDO to determine if these materials could be successfully blended and electrospun; scanning electron microscopy and mechanical characterization of the resultant scaffolds followed [71]. The mats were electrospun under similar processing conditions used for the individual components alone. Stock solutions used were 100 mg/ml of PDO in HFP and 60 mg/ml of collagen (types I and III extracted from fetal calf dermis) in HFP. Scaffolds were electrospun in the following blends (PDO:collagen by weight %): 100:0, 90:10, 80:20, and 70:30; when a mixture of collagen types I and III was used, it was a 50:50 blend of the collagens. The scaffold fiber diameters for the blends ranged from 210 to 340 nm, but an increase in the percentage of collagen did not have a significant effect on mean fiber diameter (though the addition of collagen to PDO did decrease the fiber diameter compared to PDO alone). Hydrated PDO:collagen samples were able to sustain mean peak stresses between 4.6 and 6.7 MPa, mean strain to failure values between 56.5% and 186.4%, and mean tangential moduli between 7.6 and 18.0 MPa (Fig. 22). As with other composite materials, these results were not just the average of the component contributions; an as yet unexplained interaction has taken place between the polymers. These preliminary data seem to indicate that blends of PDO and collagen may match the mechanical and morphological requirements of a blood vessel's microenvironment (as was presented in the PDO section). The hydrated electrospun PDO–collagen structures achieved a modulus between the maximum modulus of elastin and the minimum modulus of collagen. The peak stress exhibited by electrospun PDO–collagen is within the range of elastin and near the lower limit of collagen. The percent strain at break range of electrospun PDO–collagen spans both the ranges of elastin and collagen, and it exceeds the upper limit of collagen. In terms of the bulk, uniaxial mechanical properties of the blended fabric proposed as a vascular prosthetic, it is important to compare them with the vascular grafting "gold" standards, *i.e.*, expanded polytetrafluoroethylene (e-PTFE) and saphenous vein as well as the native vessel (femoral artery) (Table 2). The mechanical properties of the electrospun PDO:collagen blended vascular prosthetics fall within the ranges of the corresponding values for traditional vascular materials. Human dermal fibroblasts seeded onto the PDO:collagen type III scaffolds displayed favorable cellular interactions; the cells migrated into the thickness of the scaffolds containing collagen but merely migrated on the seeded surface of the 100% PDO scaffold.

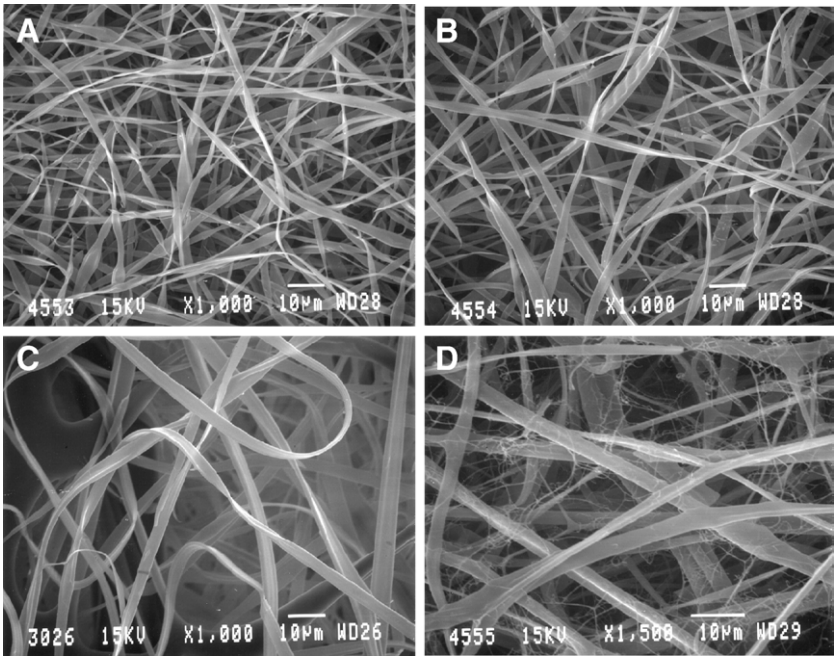

Fig. 24. Scanning electron micrographs of electrospun hemoglobin in 2,2,2-Trifluoroethanol at 150 mg/ml (A), 175 mg/ml (B), and 200 mg/ml (C) (1000× magnification). Additionally, hemoglobin and fibrinogen in a 90% HFP and 10% 10× MEM solution at a concentration of 150 mg/ml hemoglobin and 90 mg/ml fibrinogen (D) (1500× magnification).

4.11. Globular proteins

4.11.1. Fibrinogen

Wnek et al. [77] have demonstrated the feasibility of electrospinning fibrinogen to develop nanofibrous tissue engineering scaffolds, wound dressings, and hemostatic products, since fibrinogen is a soluble protein in blood plasma that has been shown to participate in wound healing as nature's provisional matrix. Scaffolds produced from concentrations of 0.083, 0.125, and 0.167 g/ml bovine fibrinogen in HFP and 10× MEM yielded fibers with diameters averaging 80±20, 310±70, and 700±110 nm, respectively (Fig. 23). The lowest concentration produced fibers with diameters within the range of fibrinogen fibers in plasma clots. Preliminary *in vitro* cell culture with neonatal rat cardiac fibroblasts proved the electrospun fibrinogen scaffolds to be extremely bioactive, with fibroblasts readily migrating through the scaffolds and depositing native collagen [78]. Uniaxial tensile testing on dry and hydrated (soaked 18 h in phosphate buffered saline at 37 °C) specimens of electrospun fibrinogen have also been performed in order to characterize their mechanical performance; with the results given in Table 3 [79]. It has also been demonstrated in our laboratory that the mechanical properties of electrospun fibrinogen scaffolds can be significantly enhanced, with no loss of bioactivity, by blending the natural polymer with PDO (unpublished lab results).

Electrospun materials composed of nanofibers have a high surface area to volume ratio. This is potentially an important consideration when designing a hemostatic product. A high surface area to volume ratio increases the surface area available for blood components to interact with to initiate clot formation. A fibrinogen scaffold with an average fiber diameter of 700 nm, dimensions 60 mm×60 mm×0.7 mm, and weighing approximately 0.08 g, has an estimated total surface area of approximately 3300 cm^2. This translates into a relative surface area to volume ratio of 1300 cm^2/cm^3 or a relative surface area to weight ratio of 4.1 m^2/g [77].

4.11.2. Hemoglobin and myoglobin

We have successfully electrospun the globular proteins hemoglobin and myoglobin [80], as well as a blend of hemoglobin and fibrinogen (unpublished data). SEMs revealed fibers with ribbon-like morphologies for electrospun hemoglobin and myoglobin. For the hemoglobin mats created, mean fiber width and thickness ranged from 2.7 to 3.6 μm and from 490 to 990 nm, respectively, with both measurements increasing with increasing polymer concentration. Additionally, surface area to volume ratios ranged between 0.50±0.16 and 1.53±0.24 m^2/cm^3 for electrospun hemoglobin fibers [80]. Using this technology, biomedical applications are readily foreseeable such as drug delivery systems, filtration systems, tissue engineering scaffolds, hemostatic bandages and wound repair treatments, and blood substitutes. Among these applications, oxygen delivery is a focus of our research since sustained wound hypoxia may be a limiting factor in the normal healing process. Electrospun scaffolds of fibrinogen and hemoglobin or myoglobin, with large surface area to volume ratios, saturated with oxygen could possibly release that oxygen (over a finite period of time) at the time of application of the dressing to the wound, thereby satisfying the local oxygen demand due to the increased metabolic rate and possibly enhancing resistance to infection. The concentration of hemoglobin or myoglobin in the scaffolds can be modified to account for the varying demands of oxygen by individual tissues and rates of cellular metabolism. This combination of natural materials would work to improve wound healing via faster cell proliferation and collagen production. Fig. 24 gives the micrographs used in the preliminary SEM analysis of the electrospun scaffolds.

5. Conclusion

Development of functional tissue engineering products requires an appropriate scaffolding to mimic the native ECM. Current research in tissue engineering is approaching a major breakthrough in the treatment of injury and disease due to the ability to routinely create ECM analogous nanofibers. Since the inception of the field of tissue engineering, many methods have evolved from the simple concept of placing cells in a degradable scaffold to building native tissues either *in vivo* or *in vitro*. These advances come on the heels of advances in the life sciences that provide critical information about the nature and development of tissues and diseases. Ultimately, engineers must match applications, materials, and fabrication processes to best meet the needs of the tissue they wish to build. It is anticipated that nanotechnology will be a key component in the development of the next generation of scaffolds, particularly with respect to the fabrication component.

References

[1] R. Langer, J.P. Vacanti, Tissue engineering, Science 260 (1993) 920–926.
[2] J.P. Vacanti, C.A. Vacanti, The challenge of tissue engineering, in: R. Lanza, R. Langer, W. Chick (Eds.), Principles of Tissue Engineering, Academic Press, San Diego, CA, 1997, pp. 1–5.
[3] S. Kidoaki, I.K. Kwon, T. Matsuda, Mesoscopic spatial designs of nano- and microfiber meshes for tissue-engineering matrix and scaffold based on newly devised multilayering and mixing electrospinning techniques, Biomaterials 26 (2005) 37–46.
[4] L. Huang, et al., Engineered collagen–PEO nanofibers and fabrics, Journal of Biomaterials Science. Polymer Ed. 12 (2001) 979–993.
[5] E.D. Boland, et al., Utilizing acid pretreatment and electrospinning to improve biocompatibility of poly(glycolic acid) for tissue engineering, Journal of Biomedical Materials Research 71B (2004) 144–152.
[6] K. Shields, et al., Mechanical properties and cellular proliferation of electrospun collagen type II, Tissue Engineering 10 (2004) 1510–1517.
[7] J.J. Stankus, J. Guan, W.R. Wagner, Fabrication of biodegradable elastomeric scaffolds with sub-micron morphologies, Journal of Biomedical Materials Research. Part B, Applied Biomaterials 70A (2004) 603–614.
[8] K. Jayaraman, et al., Recent advances in polymer nanofibers, Journal of Nanoscience and Nanotechnology 4 (2004) 52–65.
[9] L.A. Smith, P.X. Ma, Nano-fibrous scaffolds for tissue engineering, Colloids and Surfaces. B, Biointerfaces 39 (2004) 125–131.
[10] X. Wen, D. Shi, N. Zhang, Applications of nanotechnology in tissue engineering, in: H. Nalwa (Ed.), Handbook of Nanostructured Biomaterials and their Applications in Nanobiotechnology, American Scientific Publishers, Stevenson Ranch, CA, 2005, pp. 1–23.
[11] Z. Ma, et al., Potential of nanofiber matrix as tissue-engineering scaffolds, Tissue Engineering 11 (2005) 101–109.
[12] J.D. Hartgerink, E. Beniash, S.I. Stupp, Self-assembly and mineralization of peptide-amphiphile nanofibers, Science 294 (2001) 1684–1688.

[13] S. Zhang, Fabrication of novel biomaterials through molecular self-assembly, Nature Biotechnology 21 (2003) 1171–1178.
[14] J.D. Hartgerink, E. Beniash, S.I. Stupp, Peptide-amphiphile nanofibers: a versatile scaffold for the preparation of self-assembling materials, Proceedings of the National Academy of Sciences of the United States of America 99 (2002) 5133–5138.
[15] V.J. Chen, P.X. Ma, Nano-fibrous poly(-lactic acid) scaffolds with interconnected spherical macropores, Biomaterials 25 (2004) 2065–2073.
[16] P.X. Ma, R. Zhang, Synthetic nano-scale fibrous extracellular matrix, Journal of Biomedical Materials Research 46 (1999) 60–72.
[17] R. Zhang, P.X. Ma, Synthetic nano-fibrillar extracellular matrices with predesigned macroporous architectures, Journal of Biomedical Materials Research. Part B, Applied Biomaterials 52 (2000) 430–438.
[18] D.H. Reneker, I. Chun, Nanometre diameter fibres of polymer, produced by electrospinning, Nanotechnology 7 (1996) 216–223.
[19] S. Liao, B. Li, Z. Ma, H. Wei, C. Chan, S. Ramakrishna, Biomimetic electrospun nanofibers for tissue regeneration, Biomedical Materials 1 (2006) R45–R53.
[20] E.D. Boland, et al., Tissue engineering scaffolds, in: G.L. Bowlin, G.E. Wnek (Eds.), The Encyclopedia of Biomaterials and Biomedical Engineering, Marcel Dekker, Inc., New York, 2004, pp. 1630–1638.
[21] Z.M. Huang, et al., A review on polymer nanofibers by electrospinning and their applications in nanocomposites, Composites Science and Technology 63 (2003) 2223–2253.
[22] D. Li, Y. Xia, Electrospinning of nanofibers: reinventing the wheel? Advanced Materials 16 (2004) 1151–1170.
[23] S. Ramakrishna, et al., Introduction to Electrospinning and Nanofibers, World Scientific Publishing Company, Incorporated, 2005.
[24] J. Lannutti, D. Reneker, T. Ma, D. Tomasko, D. Farson, Electrospinning for tissue engineering scaffolds, Materials Science & Engineering. C, Biomimetic and Supramolecular Systems 27 (2007) 504–509.
[25] Q.P. Pham, U. Sharma, A.G. Mikos, Electrospinning of polymeric nanofibers for tissue engineering applications: a review, Tissue Engineering 12 (2006) 1197–1211.
[26] M. Bognitzki, et al., Nanostructured fibers via electrospinning, Advanced Materials 13 (2001) 70–72.
[27] M. Martins-Green, The dynamics of cell–ECM interactions with implications for tissue engineering, in: R. Lanza, R. Langer, W. Chick (Eds.), Principles of Tissue Engineering, Academic Press, San Diego, CA, 1997, pp. 23–46.
[28] M.J. Humphries, The molecular basis and specificity of integrin–ligand interactions, Journal of Cell Science 97 (1990) 585–592.
[29] B. Palsson, S. Bhatia, Tissue Engineering, 1 ed., Pearson Prentice Hall, Upper Saddle River, NJ, 2004, pp. 117–124.
[30] B.R. Olsen, Matrix molecules and their ligands, in: R. Lanza, R. Langer, W. Chick (Eds.), Principles of Tissue Engineering, R. D. Landes Company, 1997, pp. 47–65.
[31] F. Grinnell, Cell–collagen interactions: overview, Methods Enzymol. Academic Press, 1982, pp. 499–503.
[32] S.F. Badylak, The extracellular matrix as a scaffold for tissue reconstruction, Seminars in Cell & Developmental Biology 13 (2002) 377–383.
[33] P.P. Reddy, et al., Regeneration of functional bladder substitutes using large segment acellular matrix allografts in a porcine model, The Journal of Urology 164 (2000) 936–941.
[34] W.H. Wong, D.J. Mooney, Synthesis and properties of biodegradable polymers used as synthetic matrices for tissue engineering, in: A. Atala, et al., (Eds.), Synthetic Biodegradable Polymer Scaffold, Birhauser, Boston, 1997, pp. 50–82.
[35] E.D. Boland, et al., Electrospinning of bioresorbable polymers for tissue engineering scaffolds, in: D.H. Reneker, H. Fong (Eds.), Polymeric Nanofibers, Oxford University Press, New York, 2006, pp. 188–204.
[36] T. Barrows, Synthetic bioabsorbable polymers, in: S. M (Ed.), High Performance Biomaterials: a Comprehensive Guide to Medical and Pharmaceutical Applications, Technomics, Lancaster, 1991, pp. 243–257.
[37] C.C. Chu, A. Browning, The study of thermal and gross morphologic properties of polyglycolic acid upon annealing and degradation treatments, Journal of Biomedical Materials Research 22 (1988) 699–712.
[38] D. Mooney, R. Langer, Engineering biomaterials for tissue engineering: the 10–100 micron size scale, in: J. Bronzino (Ed.), The Biomedical Engineering Handbook, CRC Press, Boca Raton, 1995, pp. 1609–1618.
[39] E.D. Boland, G.E. Wnek, G.L. Bowlin, Poly(glycolic acid), The Encyclopedia of Biomaterials and Biomedical Engineering, in: G.L. Bowlin, G.E. Wnek (Eds.), Marcel Dekker, Inc., New York, 2004, pp. 1246–1253.
[40] E.D. Boland, et al., Tailoring tissue engineering scaffolds using electrostatic processing techniques: a study of poly(glycolic acid) electrospinning, Journal of Macromolecular Science. Pure and Applied Chemistry 38 (2001) 1231–1243.
[41] Y. You, et al., In vitro degradation behavior of electrospun polyglycolide, polylactide, and poly(lactide-co-glycolide), Journal of Applied Polymer Science 95 (2005) 193–200.
[42] F. Yang, et al., Electrospinning of nano/micro scale poly(L-lactic acid) aligned fibers and their potential in neural tissue engineering, Biomaterials 26 (2005) 2603–2610.
[43] Y.H. Lee, et al., Electrospun dual-porosity structure and biodegradation morphology of Montmorillonite reinforced PLLA nanocomposite scaffolds, Biomaterials 26 (2005) 3165–3172.
[44] J. Zeng, et al., Biodegradable electrospun fibers for drug delivery, Journal of Controlled Release 92 (2003) 227–231.
[45] L.I. Ramdhanie, et al., Thermal and mechanical properties of electrospun blends of poly(lactic acid) and poly(glycolic acid), Polymer Journal 38 (2006) 1137–1145.
[46] J.D. Stitzel, et al., Arterial smooth muscle cell proliferation on a novel biomimicking, biodegradable vascular graft scaffold, Journal of Biomaterials Applications 15 (2001) 1–12.
[47] K. Kim, et al., Control of degradation rate and hydrophilicity in electrospun non-woven poly(-lactide) nanofiber scaffolds for biomedical applications, Biomaterials 24 (2003) 4977–4985.
[48] X. Zong, et al., Structure and morphology changes during in vitro degradation of electrospun poly(glycolide-co-lactide) nanofiber membrane, Biomacromolecules 4 (2003) 416–423.
[49] W.J. Li, et al., Electrospun nanofibrous structure: a novel scaffold for tissue engineering, Journal of Biomedical Materials Research 60 (2002) 613–621.
[50] X. Zong, et al., Electrospun fine-textured scaffolds for heart tissue constructs, Biomaterials 26 (2005) 5330–5338.
[51] D.S. Katti, et al., Bioresorbable nanofiber-based systems for wound healing and drug delivery: optimization of fabrication parameters, Journal of Biomedical Materials Research. Part B, Applied Biomaterials 70B (2004) 286–296.
[52] E.D. Boland, et al., Electrospinning polydioxanone for biomedical applications, Acta Biomaterialia 1 (2005) 115–123.
[53] W.M. Abbott, R.P. Cambria, Control of physical characteristics (elasticity and compliance) of vascular grafts, in: J.C. Stanley (Ed.), Biological and Synthetic Vascular Prostheses, Grune and Stratton, New York, NY, 1982, pp. 189–220.
[54] H. Yoshimoto, et al., A biodegradable nanofiber scaffold by electrospinning and its potential for bone tissue engineering, Biomaterials 24 (2003) 2077–2082.
[55] J. Zeng, et al., Enzymatic degradation of poly(L-lactide) and poly(epsilon-caprolactone) electrospun fibers, Macromolecular Bioscience 4 (2004) 1118–1125.
[56] D.H. Reneker, et al., Nanofiber garlands of polycaprolactone by electrospinning, Polymer 43 (2002) 6785–6794.
[57] M. Shin, et al., Contractile cardiac grafts using a novel nanofibrous mesh, Biomaterials 25 (2004) 3717–3723.
[58] K. Fujihara, M. Kotaki, S. Ramakrishna, Guided bone regeneration membrane made of polycaprolactone/calcium carbonate composite nanofibers, Biomaterials 26 (2005) 4139–4147.
[59] W.J. Li, et al., Multilineage differentiation of human mesenchymal stem cells in a three-dimensional nanofibrous scaffold, Biomaterials 26 (2005) 5158–5166.
[60] J.E. Barralet, L.L. Wallace, A.J. Strain, Tissue engineering of human biliary epithelial cells on polyglycolic acid/polycaprolactone scaffolds maintains long-term phenotypic stability, Tissue Engineering 9 (2003) 1037–1045.
[61] I. Keun Kwon, S. Kidoaki, T. Matsuda, Electrospun nano- to microfiber fabrics made of biodegradable copolyesters: structural characteristics,

mechanical properties and cell adhesion potential, Biomaterials 26 (2005) 3929–3939.
[62] C. Xu, et al., Electrospun nanofiber fabrication as synthetic extracellular matrix and its potential for vascular tissue engineering, Tissue Engineering 10 (2004) 1160–1168.
[63] L. Huang, et al., Generation of synthetic elastin-mimetic small diameter fibers and fiber networks, Macromolecules 33 (2000) 2989–2997.
[64] Y.C. Fung, Biomechanics: Mechanical Properties of Living Tissues, Springer-Verlag, New York, 1993, pp. 243–249.
[65] S.A. Sell, et al., Electrospun polydioxanone–elastin blends: potential for bioresorbable vascular grafts. Biomedical Materials: Materials for Tissue Engineering and Regenerative Medicine 1 (2006) 72–80.
[66] Y. Zhang, et al., Electrospinning of gelatin fibers and gelatin/PCL composite fibrous scaffolds, Journal of Biomedical Materials Research. Part B, Applied Biomaterials 72 (2005) 156–165.
[67] M. Li, et al., Electrospun protein fibers as matrices for tissue engineering, Biomaterials 26 (2005) 5999–6008.
[68] J.A. Matthews, et al., Electrospinning of collagen nanofibers, Biomacromolecules 3 (2002) 232–238.
[69] J.A. Matthews, et al., Electrospinning of collagen type II: a feasibility study, Journal of Bioactive and Compatible Polymers 18 (2003) 125–134.
[70] C.P. Barnes, et al., Cross-linking electrospun type II collagen tissue engineering scaffolds with carbodiimide in ethanol Tissue Engineering 13 (2007) 1593–1605.
[71] C.P. Barnes, et al., Preliminary investigation of electrospun collagen and polydioxanone for vascular tissue engineering applications International, Journal of Electrospun Nanofibers and Applications 1 (2007) 73–87.
[72] E.D. Boland, et al., Electrospinning collagen and elastin: preliminary vascular tissue engineering, Frontiers in Bioscience 9 (2004) 1422–1432.
[73] I.V. Yannas, et al., Design of an artificial skin. II. Control of chemical composition, Journal of Biomedical Materials Research 14 (1980) 107–132.
[74] R.R. Brau, I.V. Yannas, Tissue engineering skin, in: G.E. Wnek, G.L. Bowlin (Eds.), Encyclopedia of Biomaterials and Biomedical Engineering, Marcel Dekker, Inc., New York, N.Y., 2004, pp. 1652–1660.
[75] J.S. Choi, et al., Effect of organosoluble salts on the nanofibrous structure of electrospun poly(3-hydroxybutyrate-co-3-hydroxyvalerate), International Journal of Biological Macromolecules 34 (2004) 249–256.
[76] I.C. Um, et al., Electro-spinning and electro-blowing of hyaluronic acid, Biomacromolecules 5 (2004) 1428–1436.
[77] G.E. Wnek, et al., Electrospinning of nanofiber fibrinogen structures, Nano Letters 3 (2003) 213–216.
[78] M.C. McManus, E.D. Boland, D.G. Simpson, C.P. Barnes, G.L. Bowlin, Electrospun fibrinogen: feasibility as a tissue engineering scaffold in a rat cell culture model, Journal of Biomedical Materials Research, A 81 (2007) 299–309.
[79] M.C. McManus, et al., Mechanical properties of electrospun fibrinogen structures, Acta Biomaterialia 2 (2006) 19–28.
[80] C.P. Barnes, et al., Feasibility of electrospinning the globular proteins hemoglobin and myoglobin, Journal of Engineered Fibers and Fabrics 1 (2006) 16–29.
[81] J. Catanese, et al., Mechanical properties of medical grade expanded polytetrafluoroethylene: the effects of internodal distance, density, and displacement rate, Journal of Biomedical Materials Research 48 (1999) 187–192.
[82] D.L. Donovan, et al., Material and structural characterization of human saphenous vein, Journal of Vascular Surgery 12 (1990) 531–537.
[83] Y.C. Fung, Blood flow in arteries, Biodynamics: Circulation, Springer-Verlag, New York, NY, 1984, pp. 77–165.
[84] H. Yamada, Mechanical properties of circulatory organs and tissues, in: F.G. Evans (Ed.), Strength of Biological Materials, Robert E. Krieger Publishing Company, Huntington, NY, 1970, pp. 106–137.